
Week 06: Magnetoelastic Microrobots

Mahmut Selman Sakar

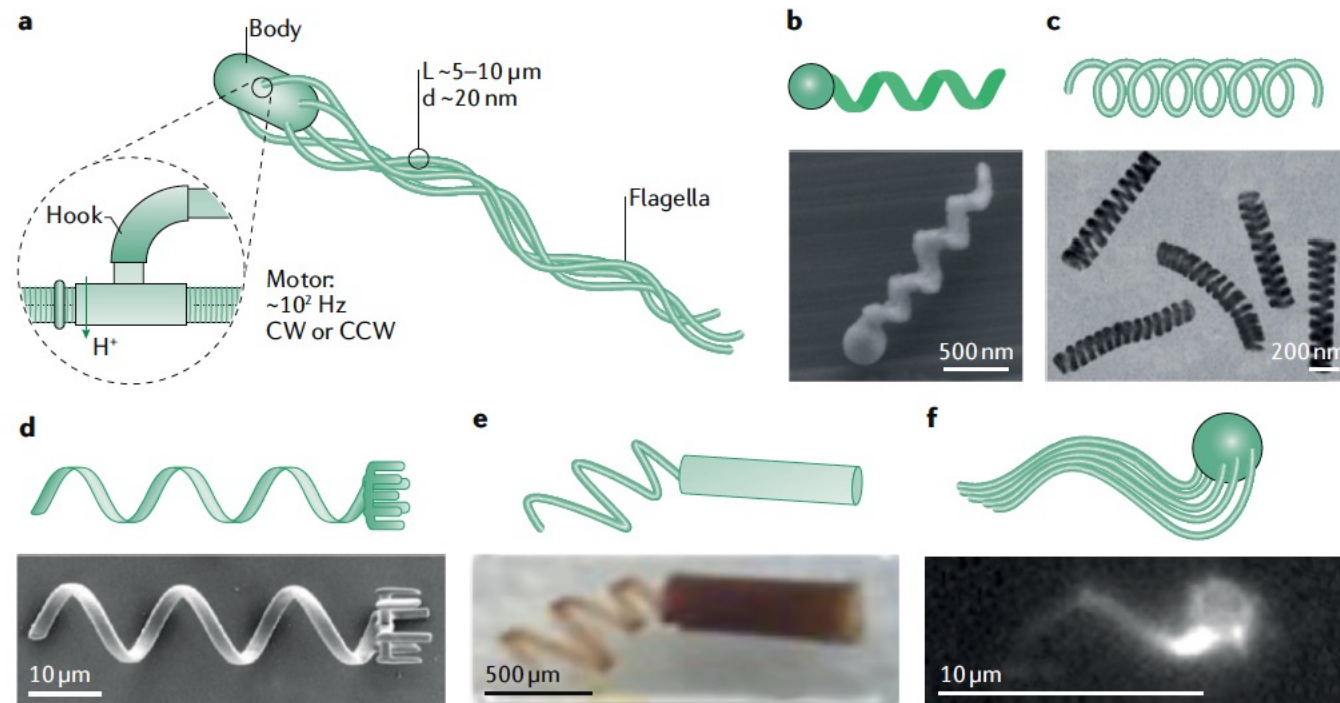
Institute of Mechanical Engineering, EPFL

Lecture Overview

- Bioinspired swimming strategies
- Magnetoelastic microrobots
- Medical instruments

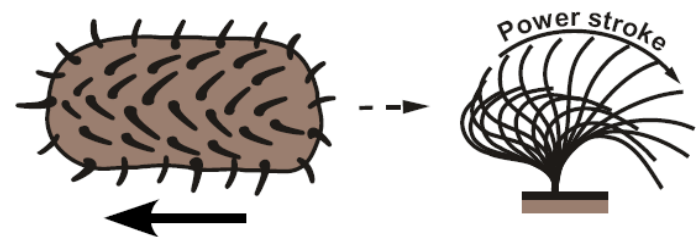
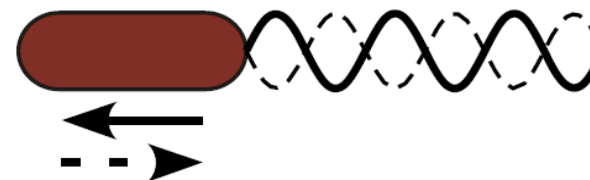
Swimming at Low Reynolds Number

- How to elude the scallop theorem (Aristotelian fluid regime)
 - Rotate a chiral arm
 - Wave an elastic arm

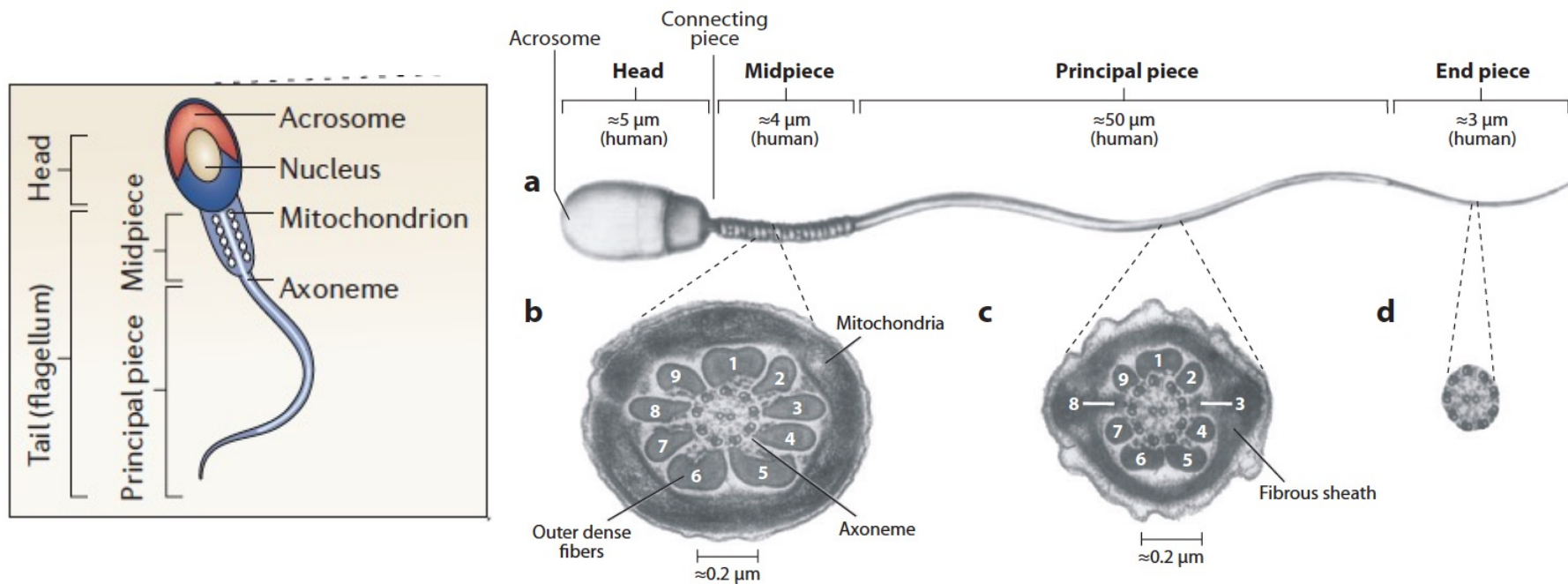


Eukaryotic Flagella and Cilia

- **Eukaryotic flagella**
 - Active organelles which create traveling waves
 - Swimming direction can be reversed by reversing the direction of the wave
 - Head-to-tail: moving forward
 - Tail-to-head: moving backwards
- **Cilia**
 - Active organelles
 - Held perpendicular during the power stroke
 - Parallel during recovery stroke



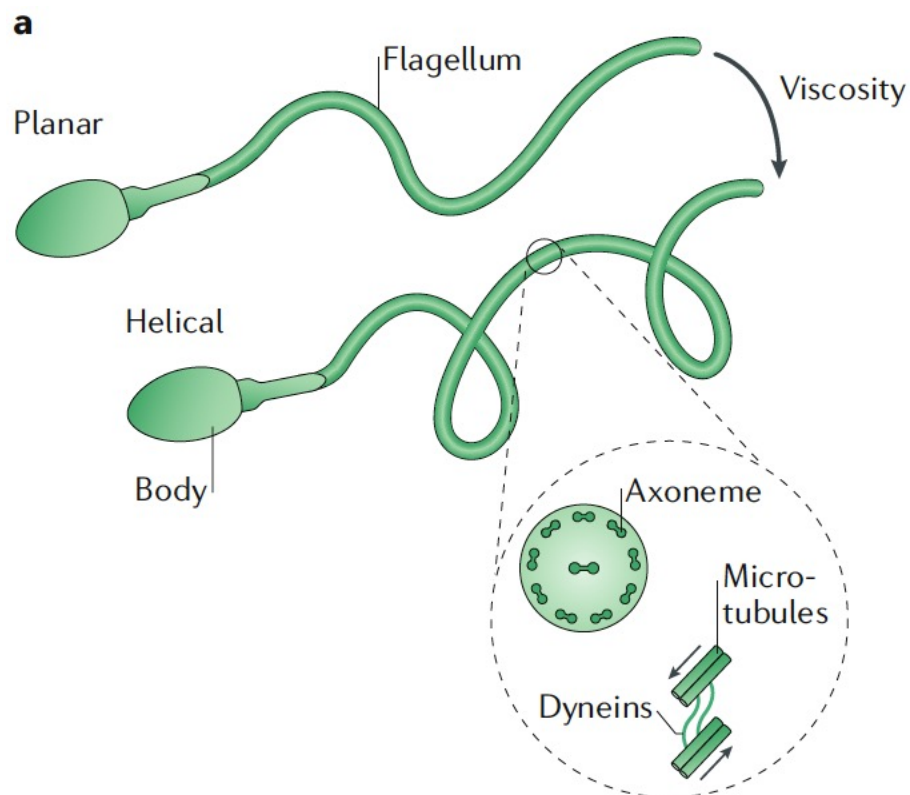
Sperm Flagella



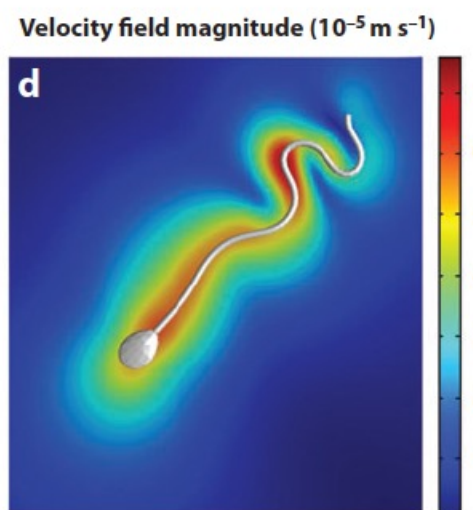
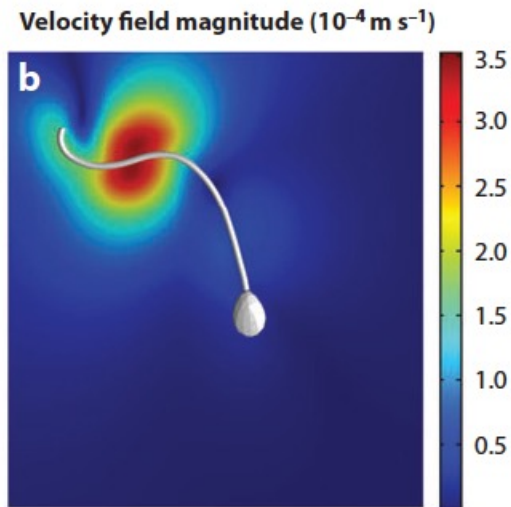
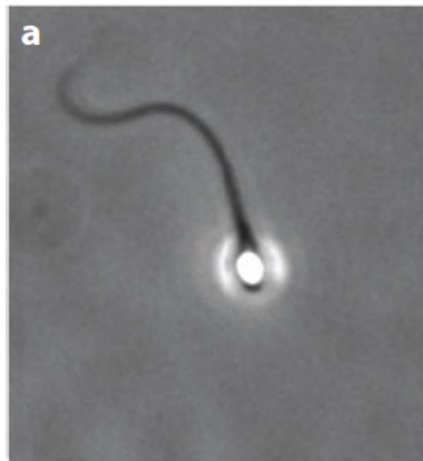
- Elastic connecting piece
- Active force arises from the action of dynein motors
- Bending wave propagating from head to the tail
- Beating frequency and waveform is modulated by calcium signaling

Eukaryotic Flagellum

- Sperm cells swim owing to bending waves that propagate along their long, flexible flagellum
- The whole tail is actuated
 - Bending is powered by dynein motor proteins that cause sliding of microtubule doublets in the axoneme
- The waveform depends on the viscosity of the surrounding fluid: planar or helical
- Long and thin flagellum
 - Guarantees asymmetry in the resistance to forward and sideways motion

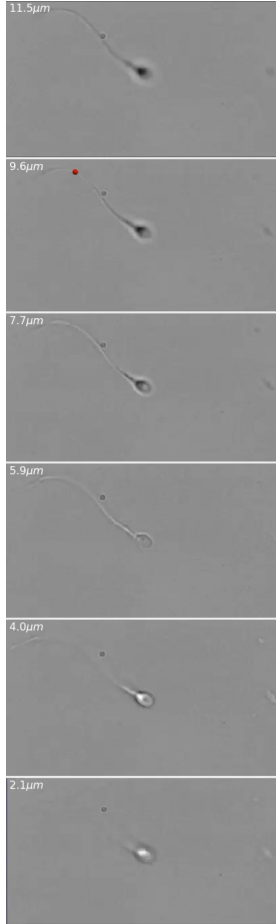


Sperm Motility ([video](#))

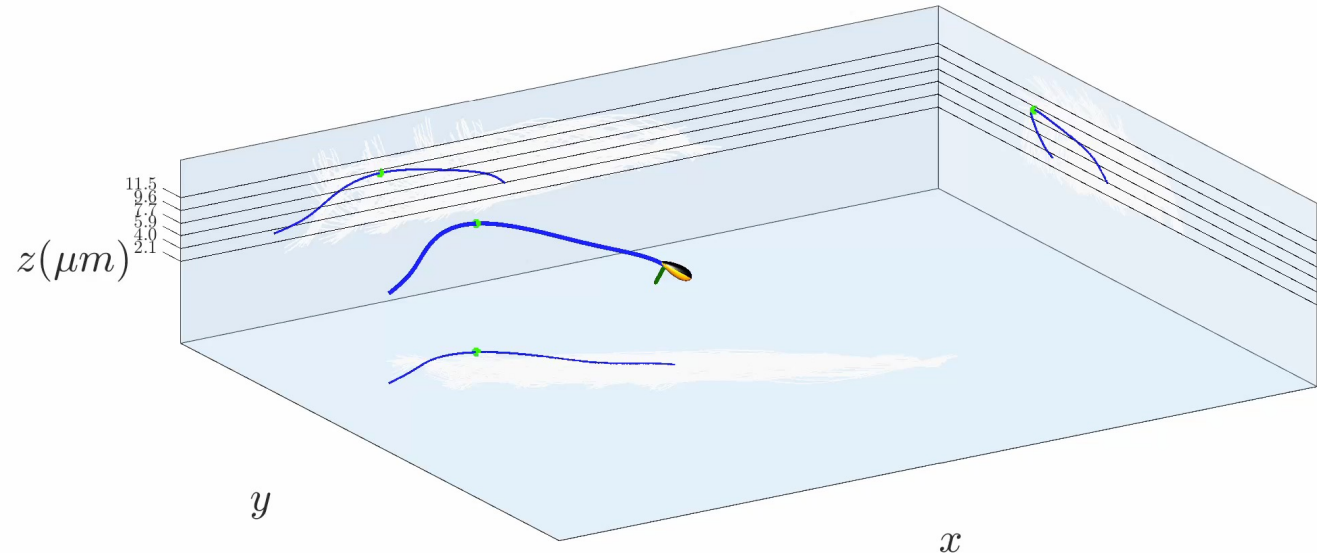


- Human sperm migrating in low and high viscosity fluids
- Boundary element method/Slender-body theory for fluid mechanics calculations
- Flow-field disturbance is an order of magnitude greater in low viscosity medium

Sperm Motility

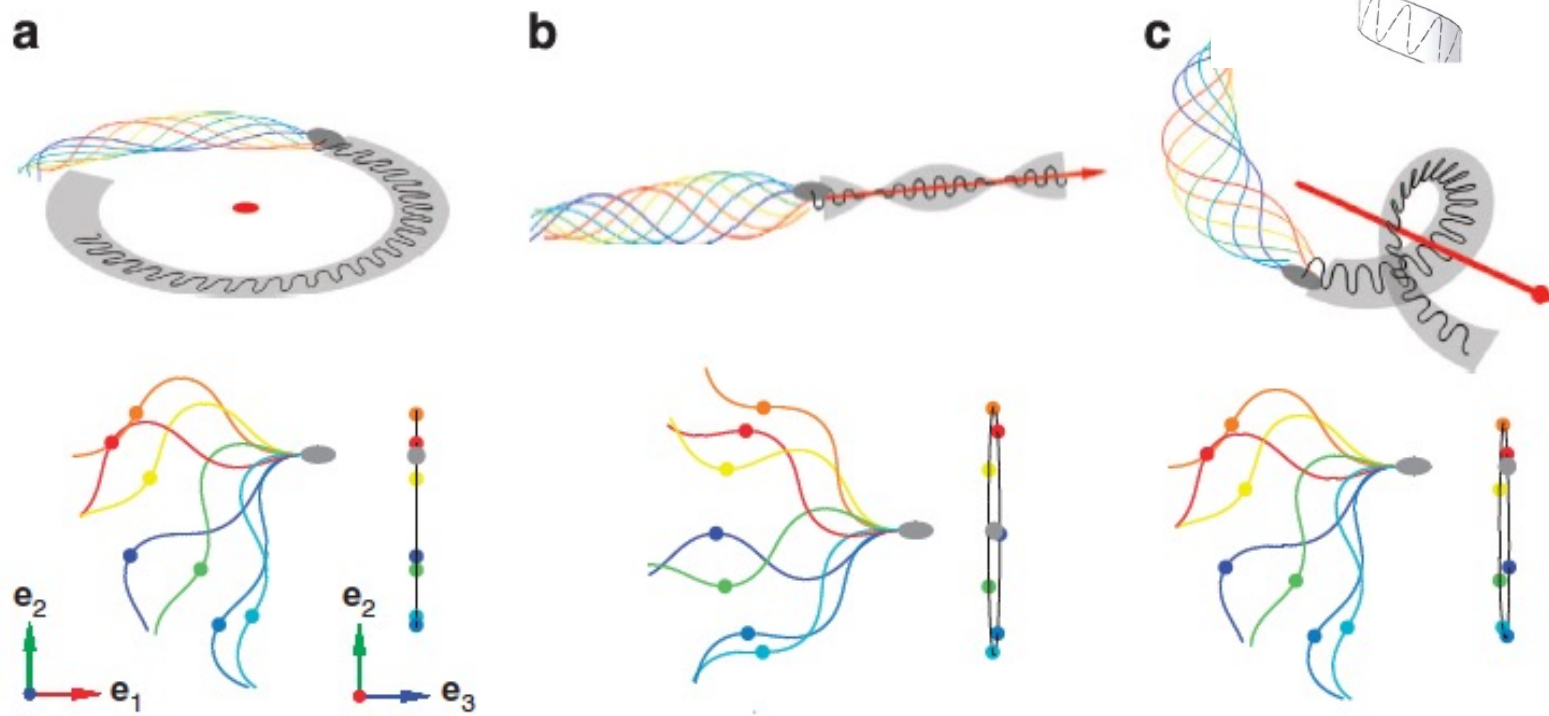
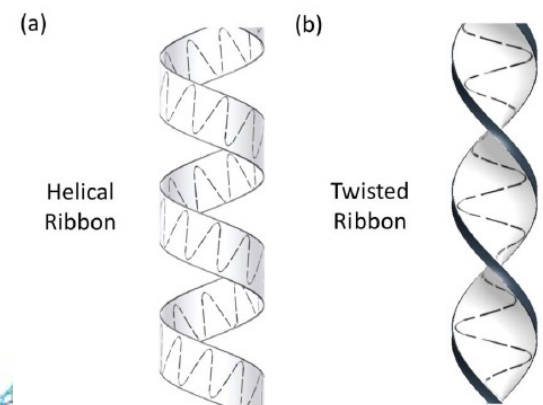


Fixed Frame - 0.01 s

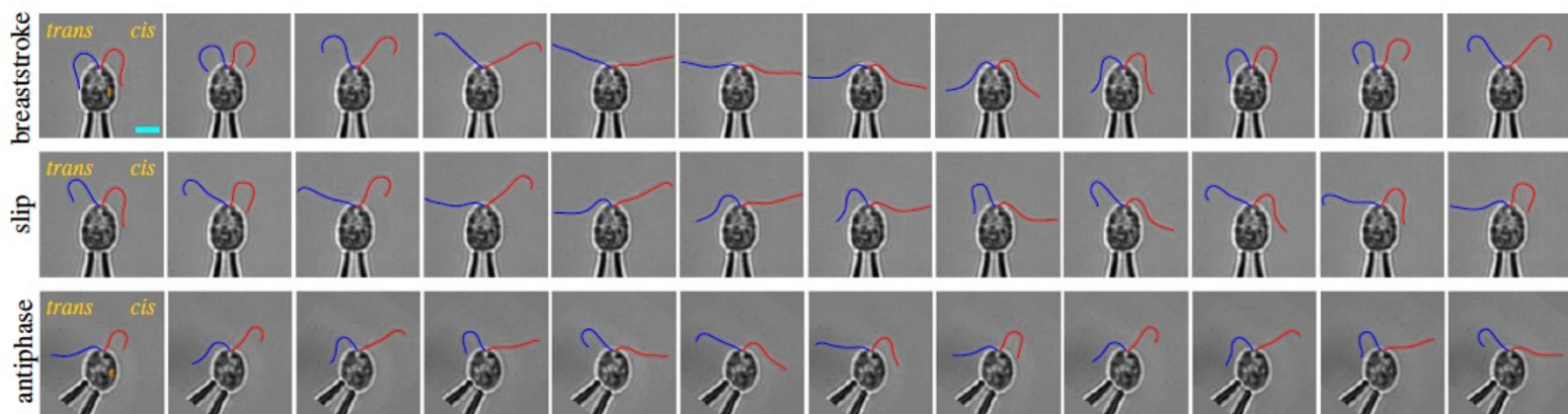
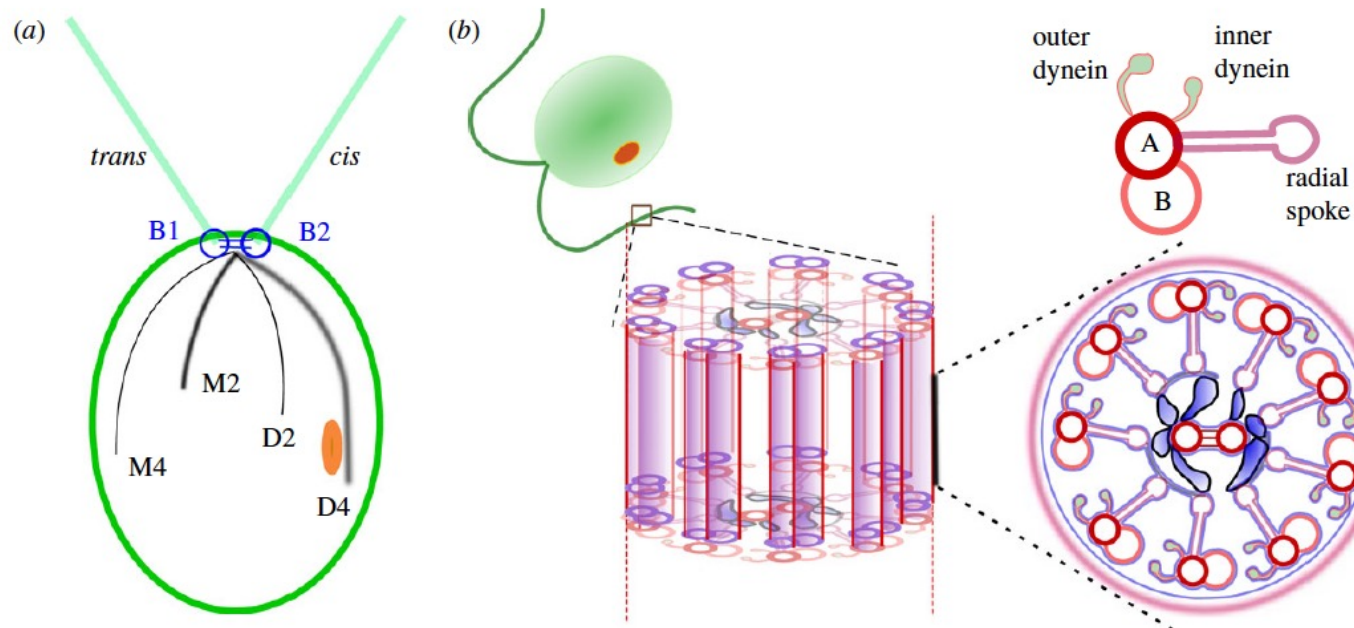


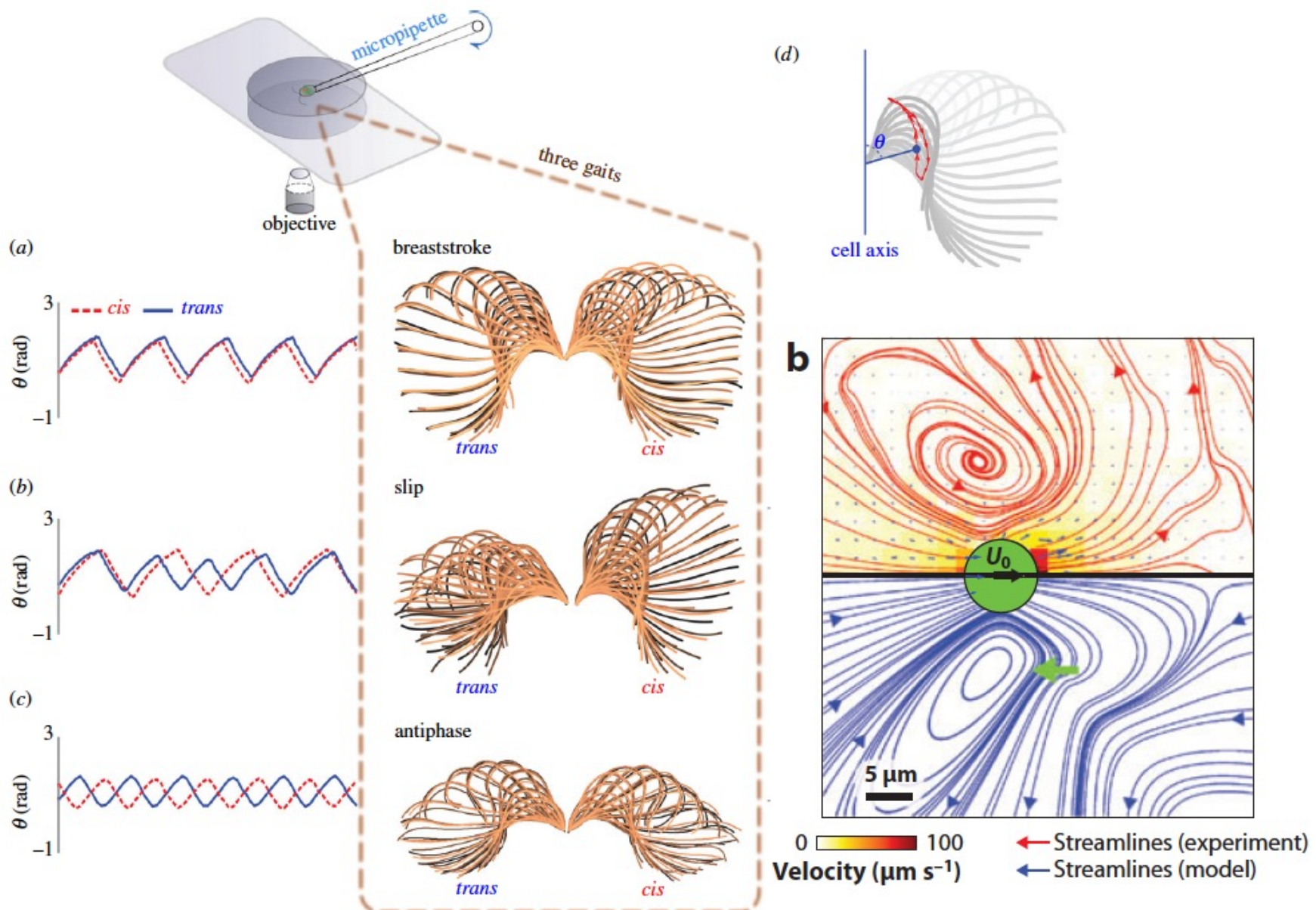
Sperm Motility

- 3D swimming pattern following helical ribbons
- Planar and asymmetric beating (a)
- Non-planar symmetric beating (b)
- Non-planar asymmetric beating (c)



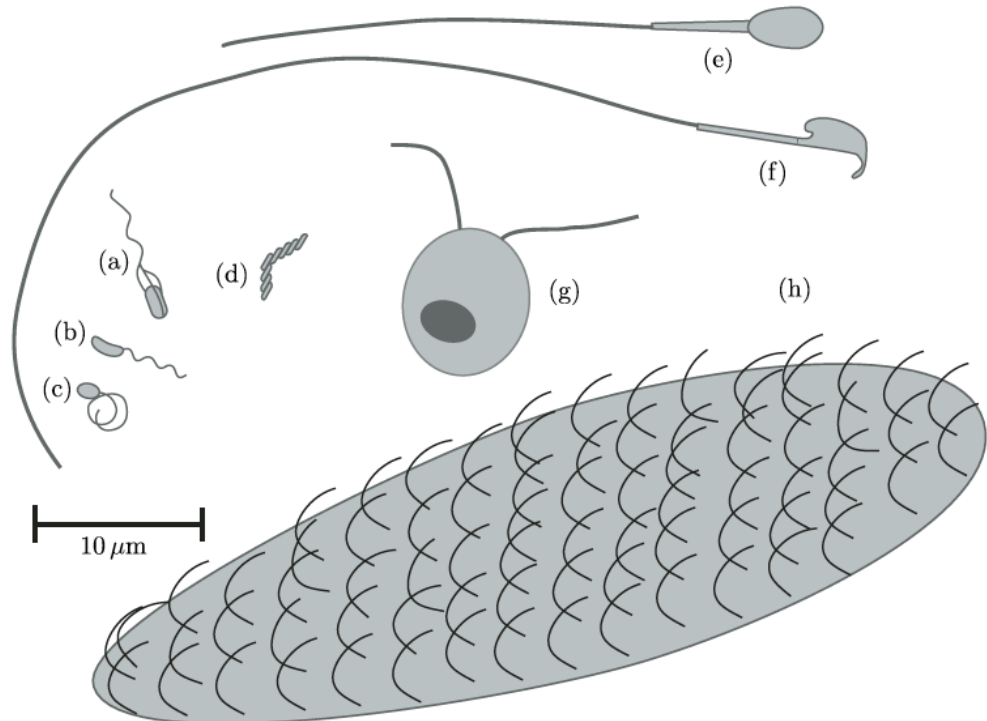
Biflagellate Alga *Chlamydomonas* [video]





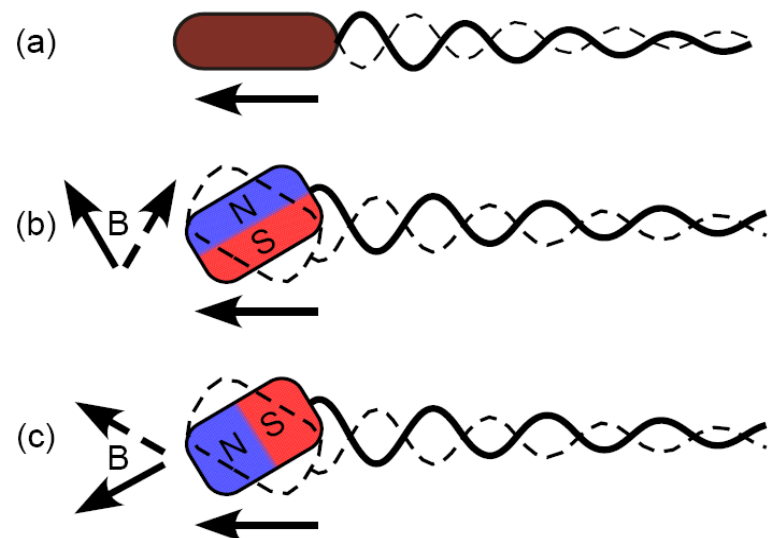
Scaling of Appendage Size

- Eukaryotic flagella are at least ten times larger (diameter and length) than bacterial flagella
 - Typical diameter: 20nm vs 200nm
- Cilia: thousands of small appendages that beat in coordinated manner
 - Propelling the cell at speeds of 500 $\mu\text{m/s}$
- With increasing size, we see a transition from flagellum to cilia

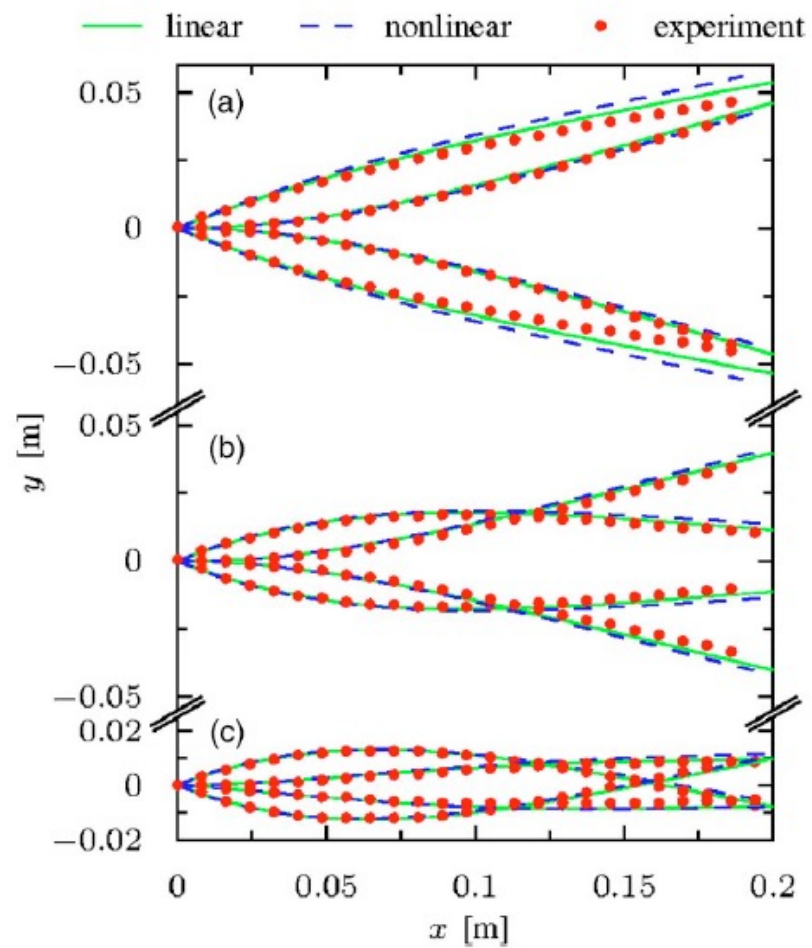
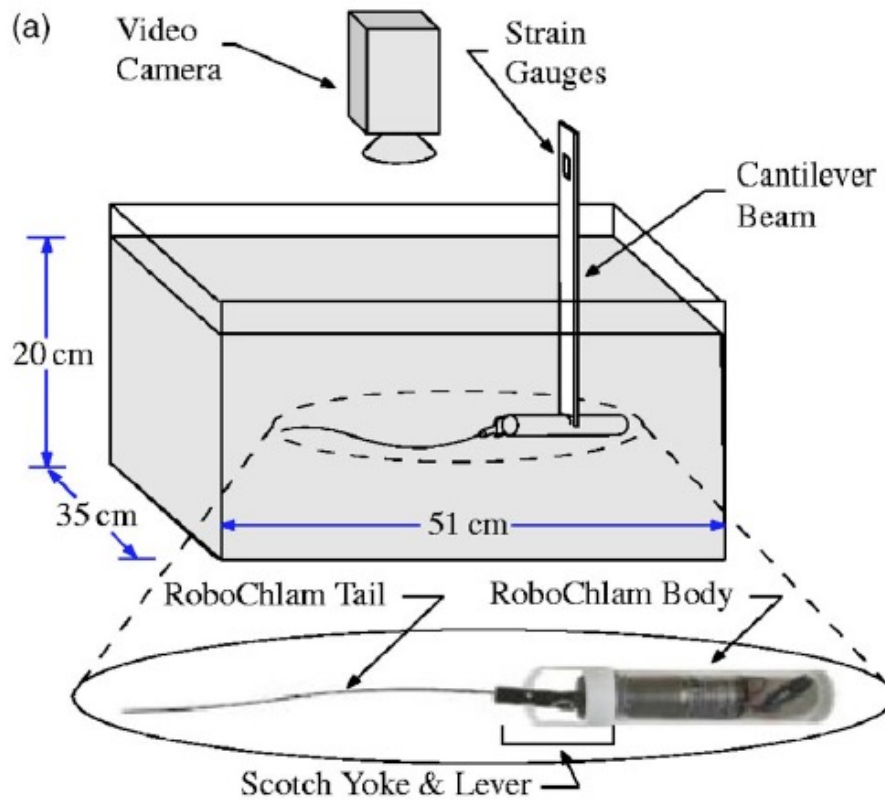


Bioinspired Swimming: Elastic Oar

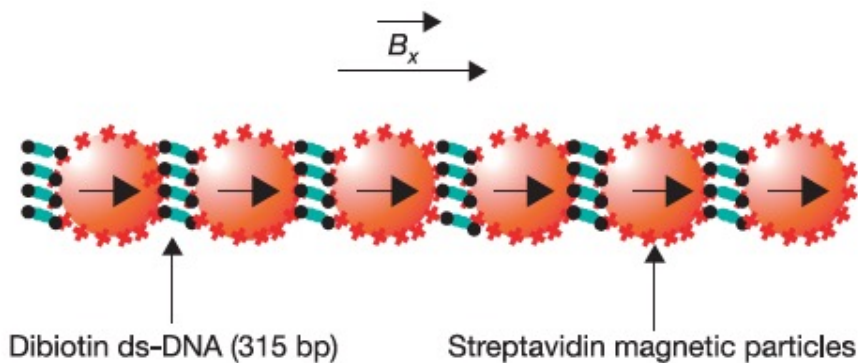
- One-sided actuation
 - There exists an optimum in tail elasticity and length
 - Too short & rigid
 - “Scallop theorem”
 - Too long & elastic
 - Increased drag
 - Use of varying magnetic fields
 - Magnetic field creates a torque on a magnet
 - By varying the field, the torque is a function of time
 - Induces a waving motion to the following tail



Flexible Oar Swimmer

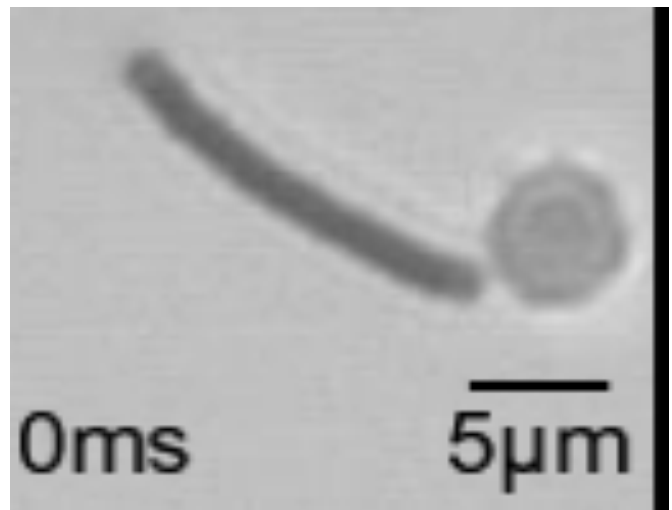
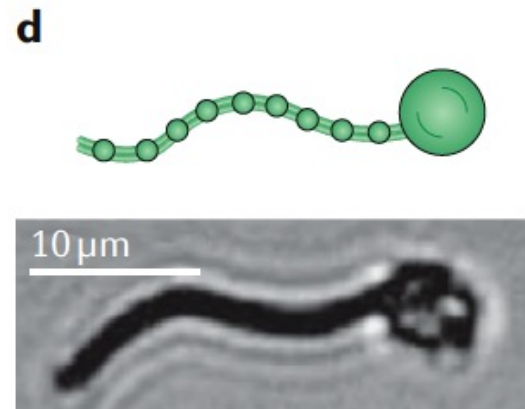


Artificial Eukaryotic Flagellum



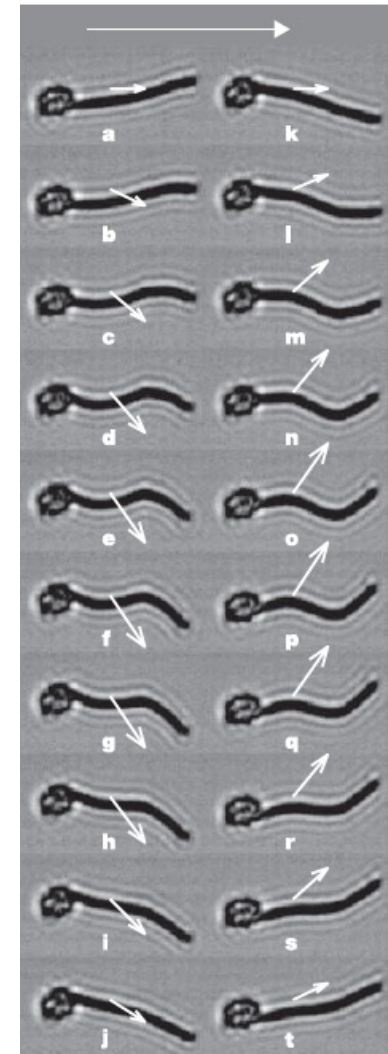
$$\mathbf{B}_x = B_x$$
$$\mathbf{B}_y = B_y \sin(2\pi ft)$$

- Magnetic microbeads
 - Each bead has an easy axis
 - They are linked with DNA
 - The beads tend to align with an oscillating external magnetic field



Artificial Eukaryotic Flagellum

- An undulation that propagates toward the attachment point from the tip of the tail
- Remember that in sperm cells bending wave propagates from head to tail



Sperm Number

- A dimensionless number that represents the relative importance of viscous to elastic stresses on a filament

$$S_p = \frac{L}{\sqrt[4]{\left(\frac{\kappa}{\xi_{\perp} \omega}\right)}}$$

L : length of the filament

κ : bending rigidity

ω : angular driving frequency

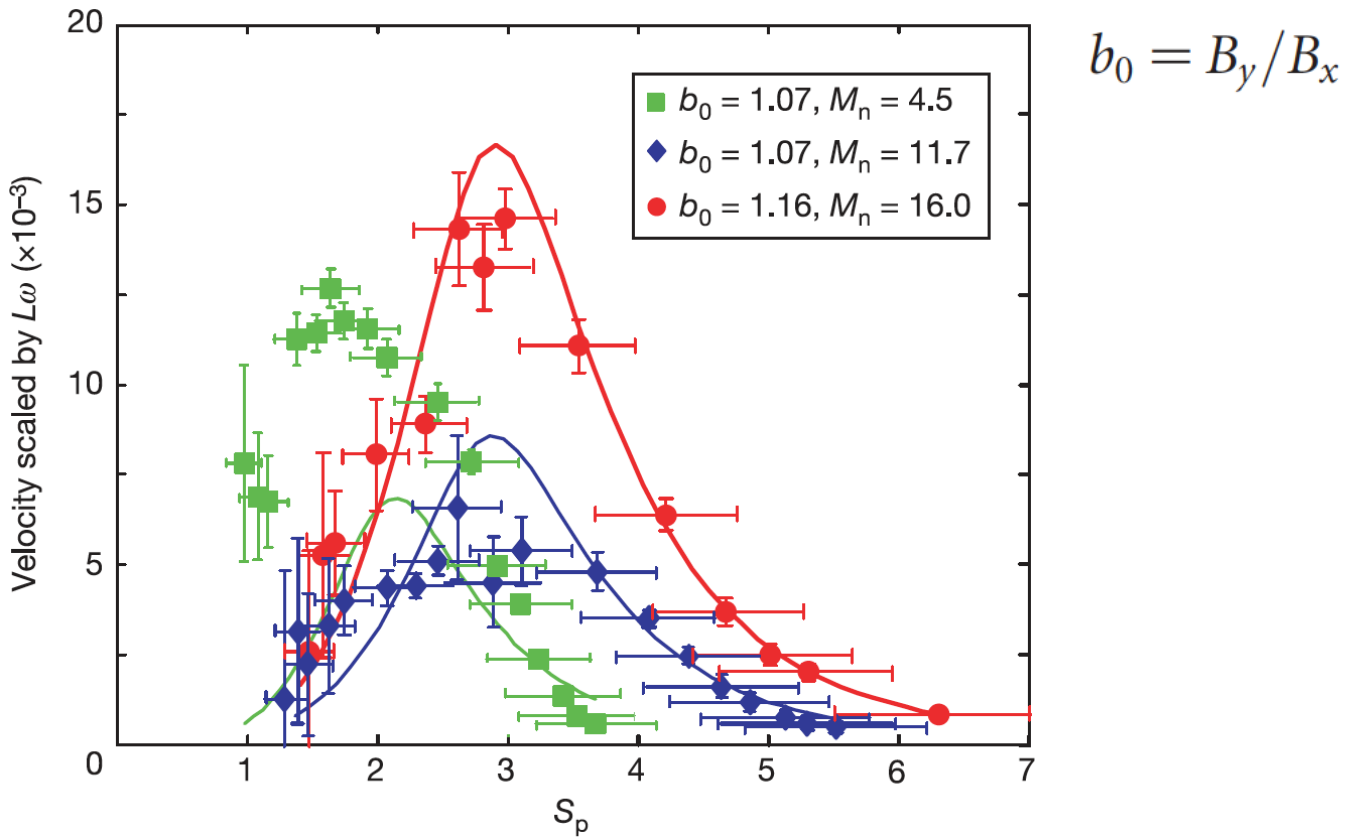
ξ_{\perp} : perpendicular viscous coefficient

- For a one-armed swimmer, two extreme regimes emerge
 - At low S_p , internal elasticity dominates
 - At high S_p , viscous friction dominates
- Maximum normalized swimming speed ($V/L\omega$) is attained for S_p of the order unity (for sperm cells $S_p = 7$)

Magnetoelastic Number and Velocity Profile

$$M_n = \frac{2\pi(aB_xL)^2}{3\mu_0\kappa} \left(\frac{\chi_{\parallel} - \chi_{\perp} + \chi_{\parallel}\chi_{\perp}/4}{(1 - \chi_{\parallel}/6)(1 + \chi_{\perp}/12)} \right)$$

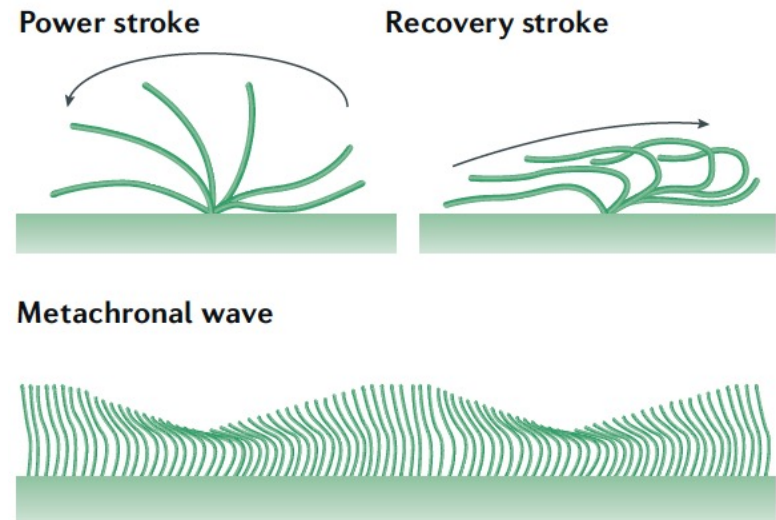
χ : magnetic susceptibility
 μ : magnetic permeability
 a : radius of the particles



$$b_0 = B_y/B_x$$

Cilia

- Found in many tissues and unicellular organisms
- Coordinated action of thousands of cilia as an effective waving surface
- **Metachronal Waves**
 - Self-organized
 - Hydrodynamic interactions
 - Not complete synchrony or randomness
 - 10-fold higher efficiency compared to cilia all beating in phase



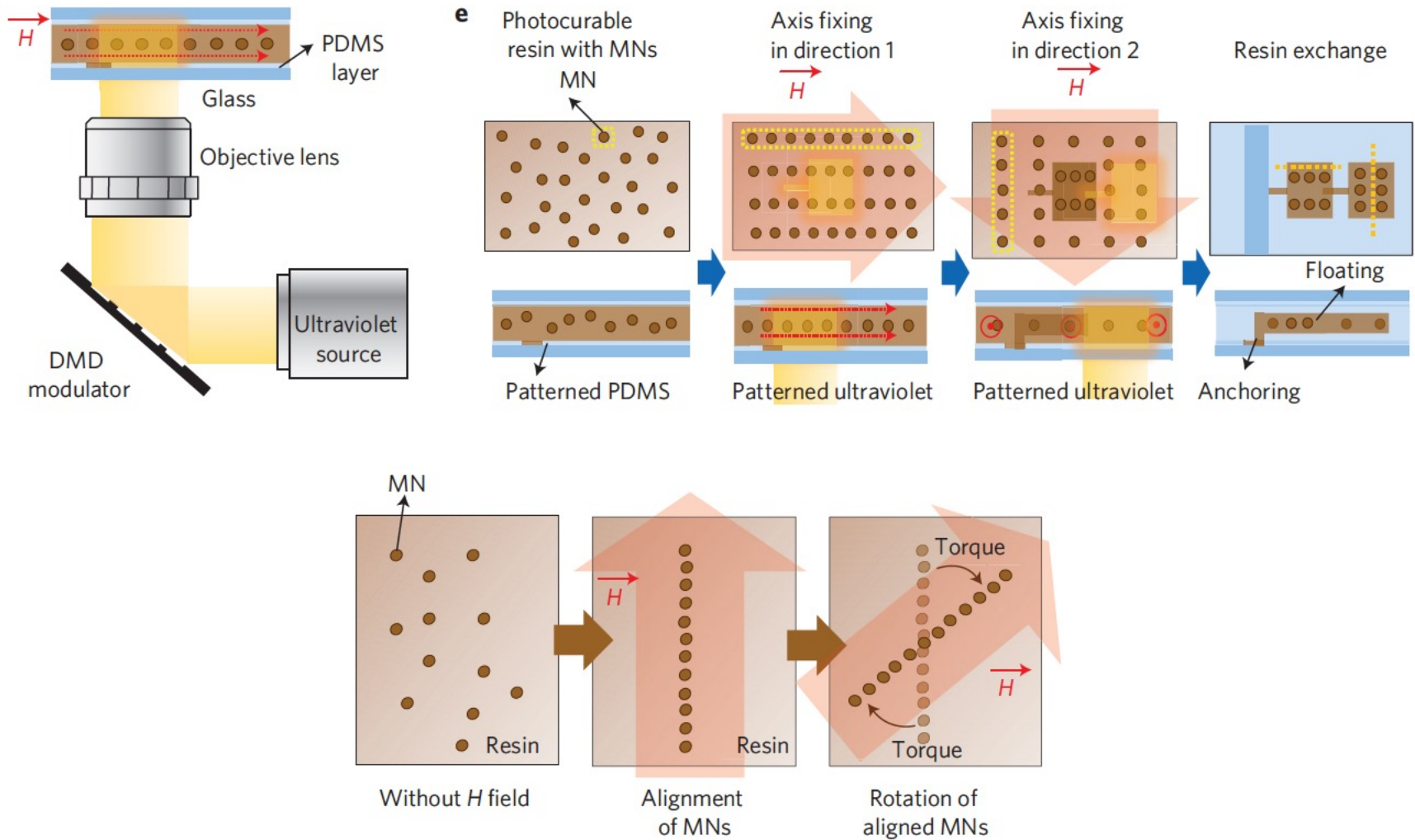
Flexible Magnetic Composites

- Magnetoreactive soft materials such as magnetorheological elastomers and ferrogels
- Under the influence of magnetic fields, the embedded particles interact with one another and with the polymer matrix
- Vibration absorbers, sensing devices, engine mounts

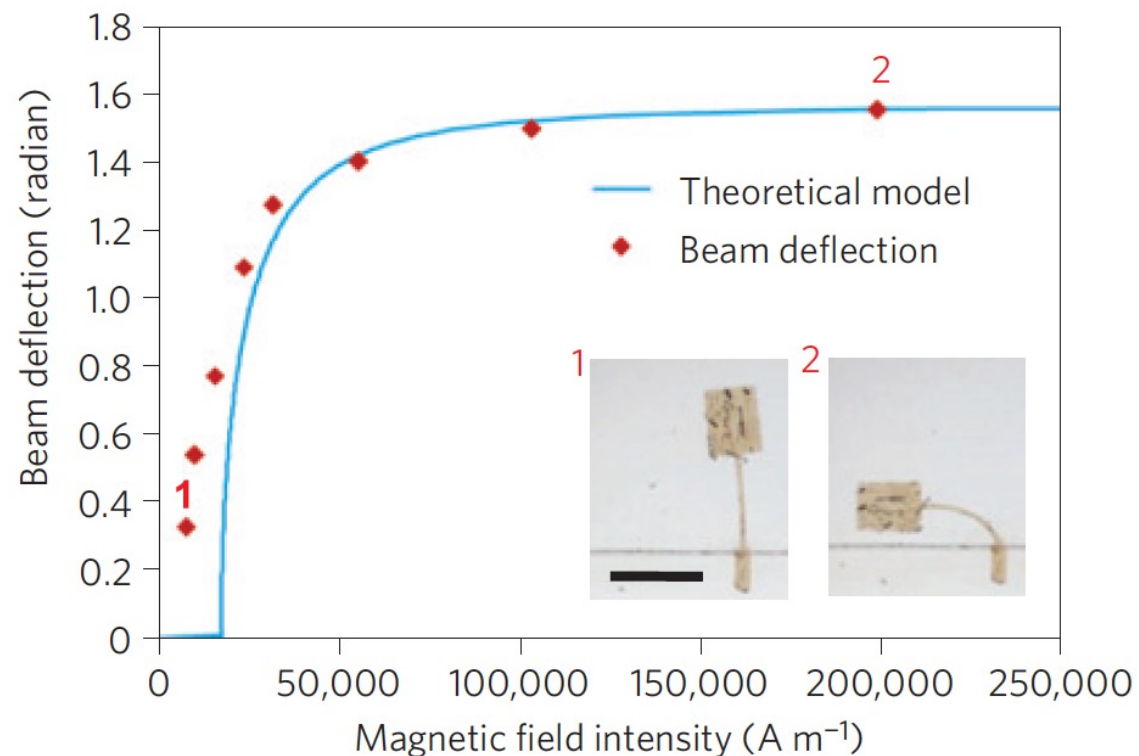
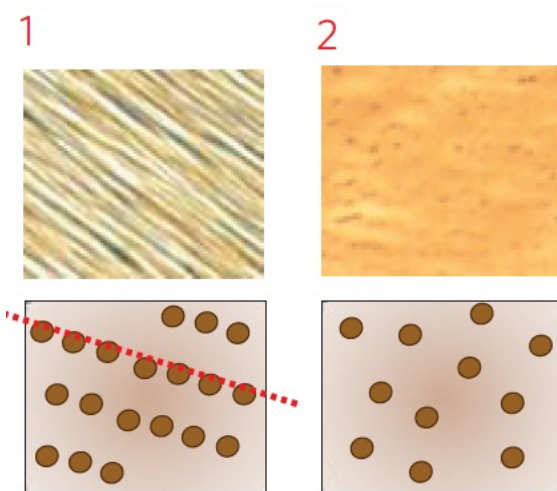
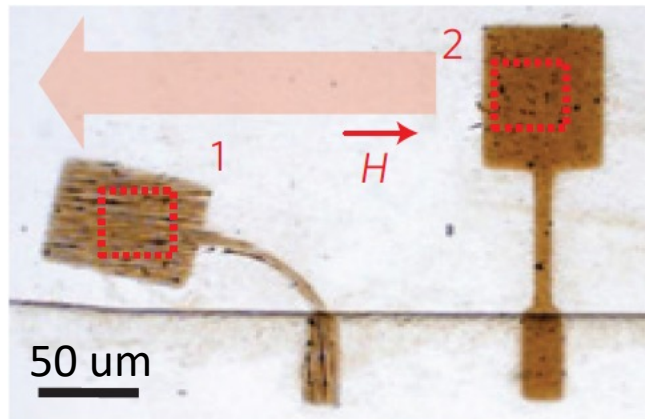
Soft Magnetic Composites

- Embedding particles of low-coercivity ferromagnetic materials in hydrogels
 - Soft magnetic materials
 - Iron and iron oxides
- Soft magnetic materials develop strong magnetization along the applied magnetic field
- They do not retain the strong magnetism once the external field is removed
- Deformation is limited to elongation or compression under magnetic field gradients

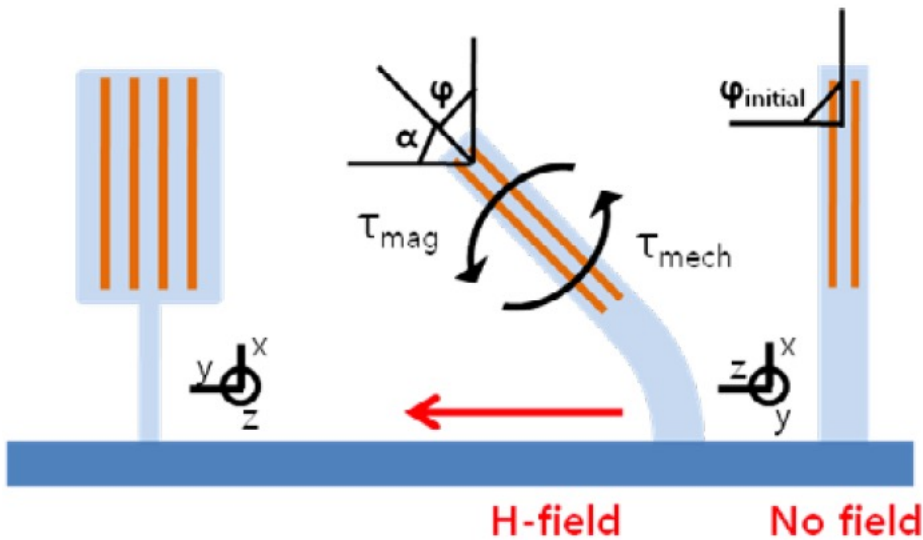
Programming magnetic anisotropy



Programming magnetic anisotropy



Programming magnetic anisotropy

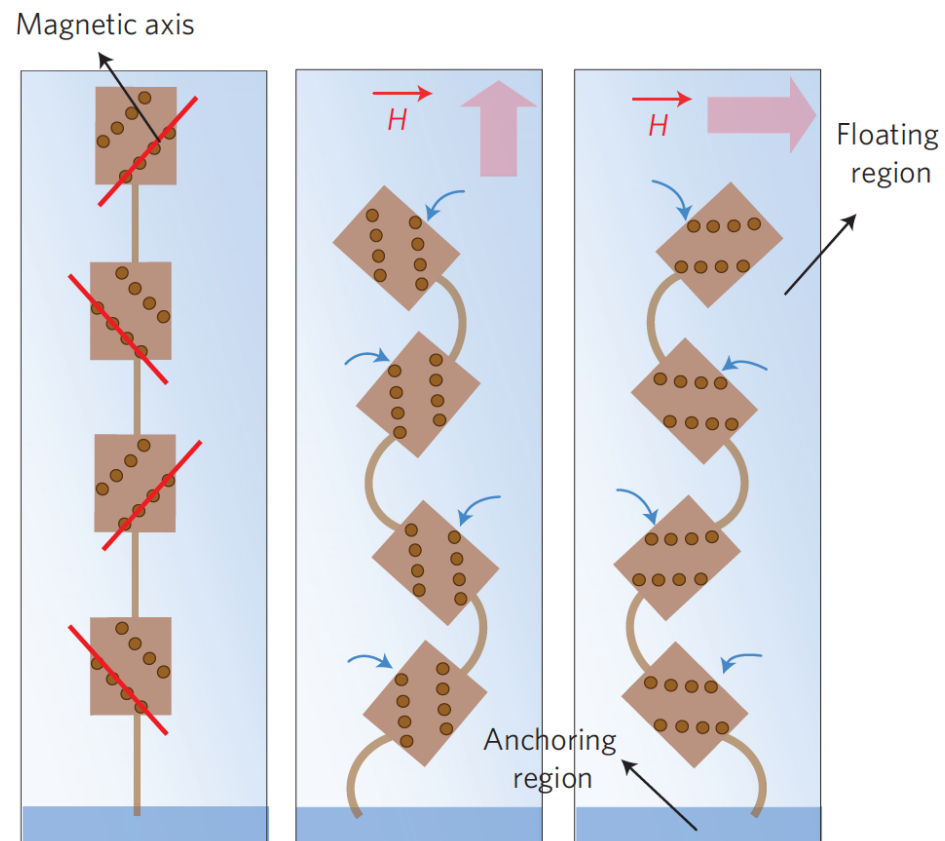
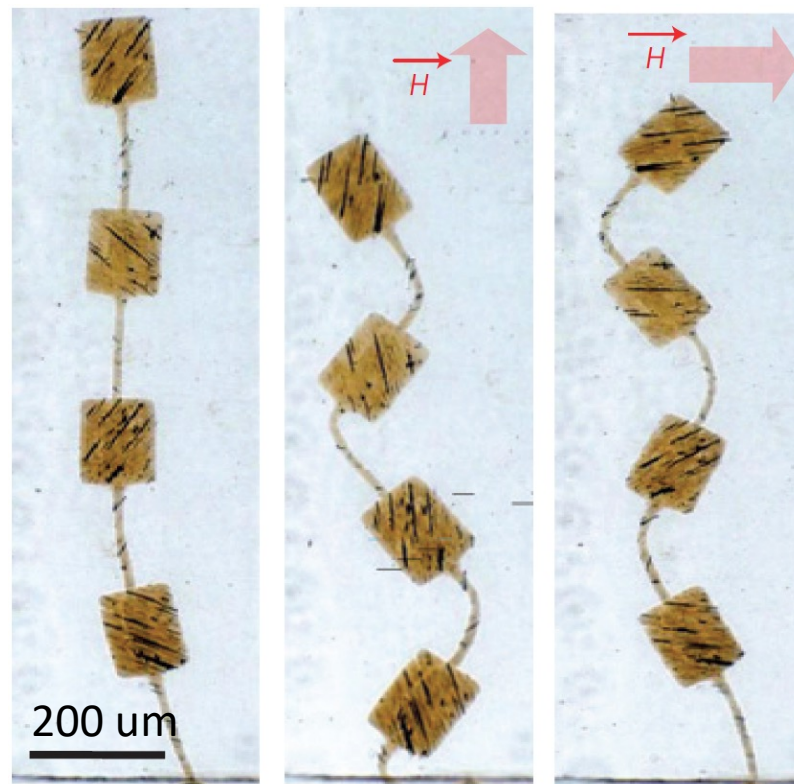
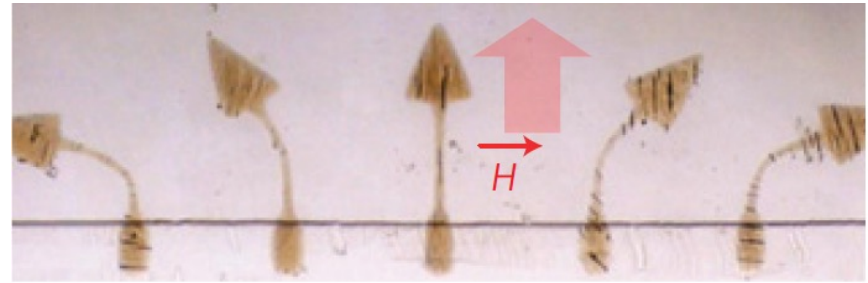
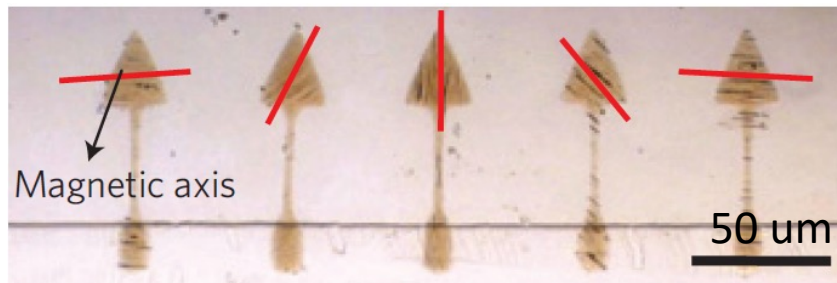


$$\tau_{mechanical} = -k_\varphi \varphi$$

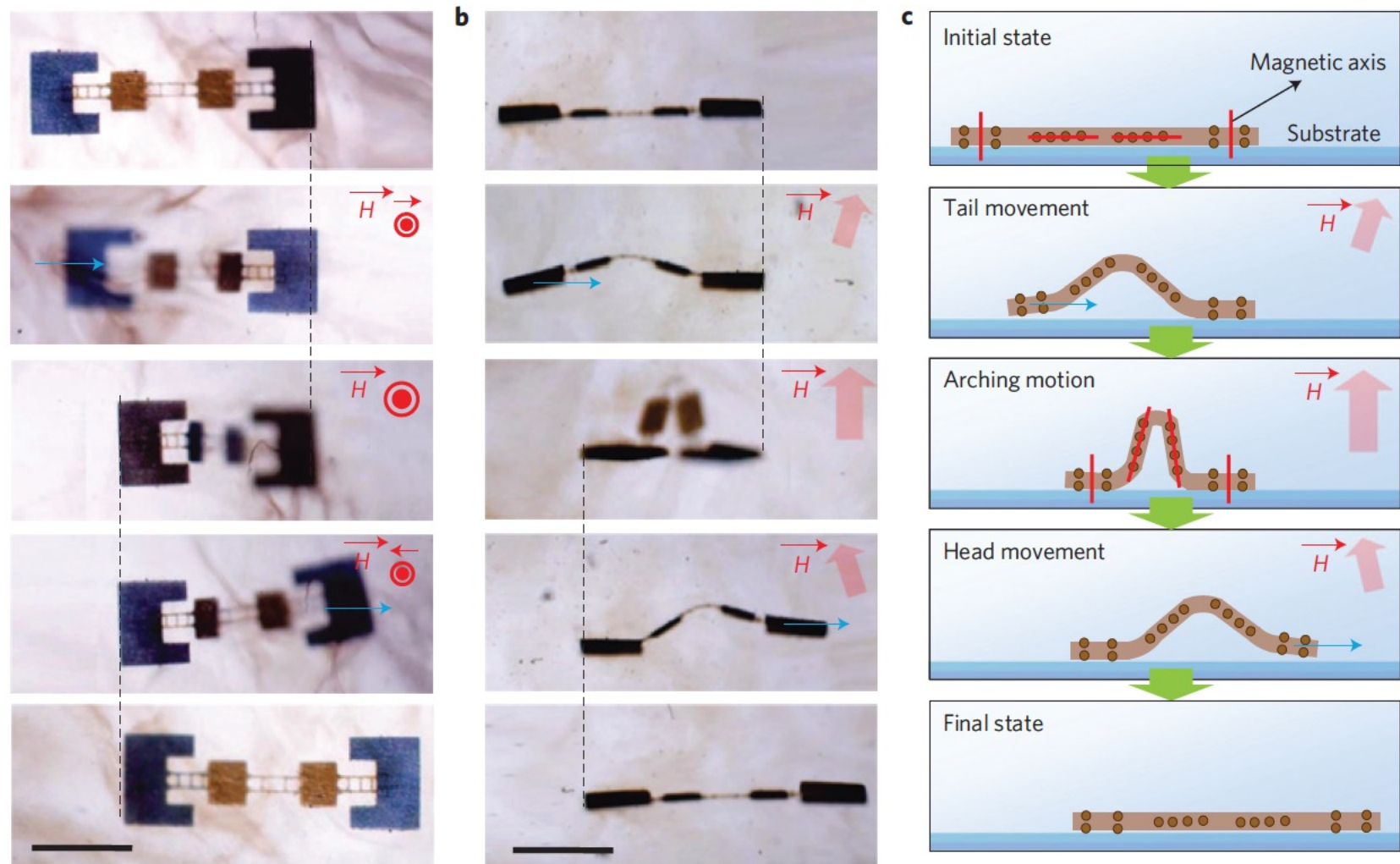
$$k_\varphi = \frac{E_y}{I} \frac{w D^3}{12}$$

$$\tau_{magnetic} = N \frac{3\mu_0 m^2}{4\pi} \sin(2\alpha) \frac{n^2}{d^3} = N \frac{3\mu_0 n^2 \chi^2 R^6 \pi}{4\pi} H^2 \sin(2\alpha)$$

Programming magnetic anisotropy

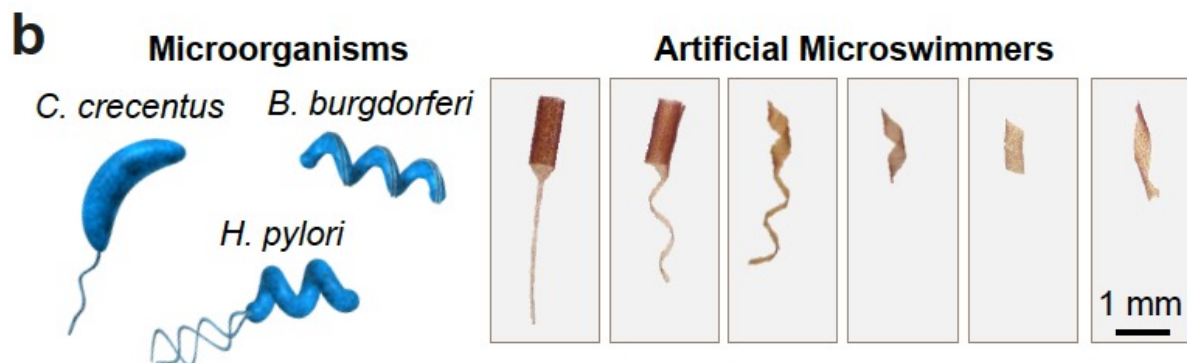
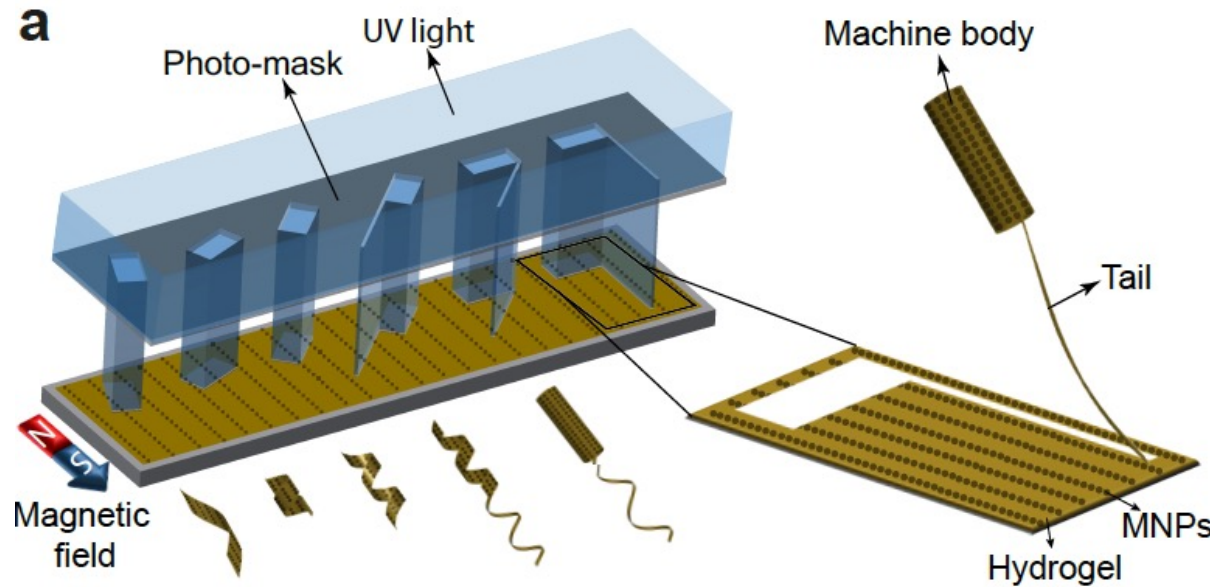


Programming magnetic anisotropy

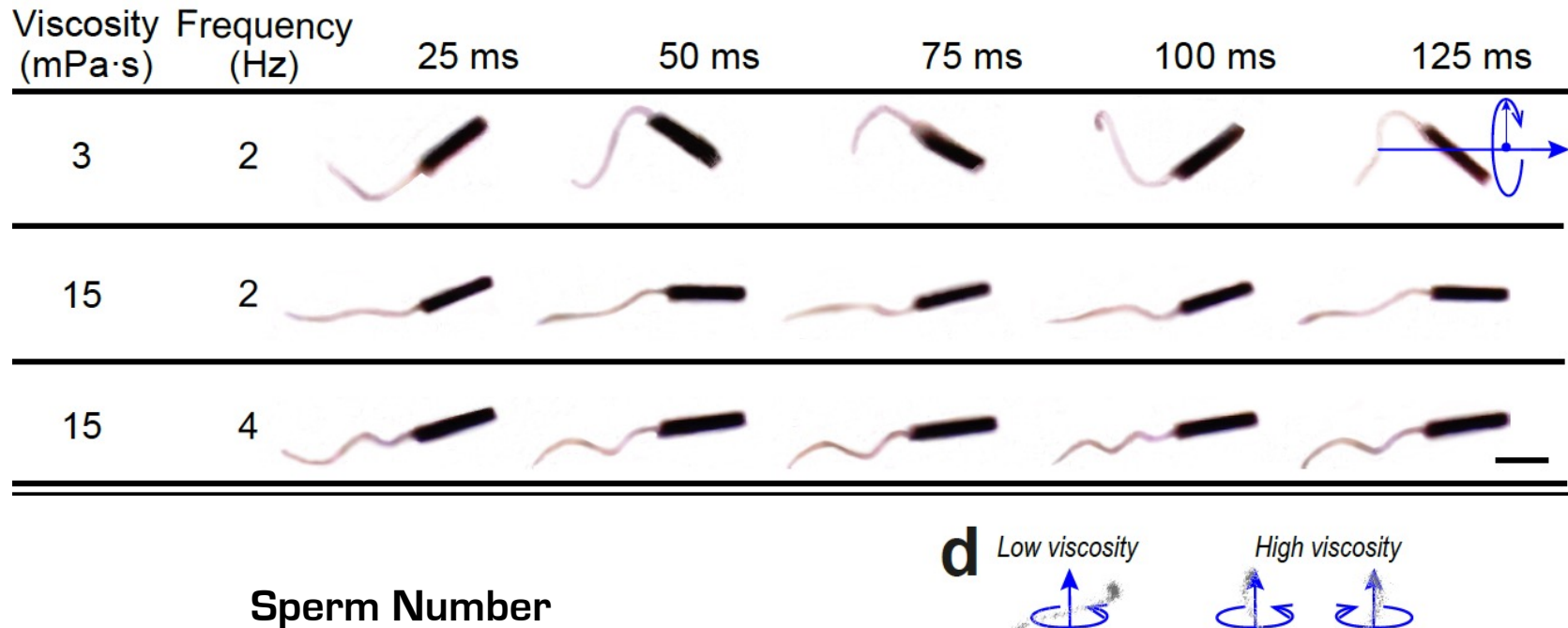


Programmable self-folding

- Differential Swelling via Particle Gradients



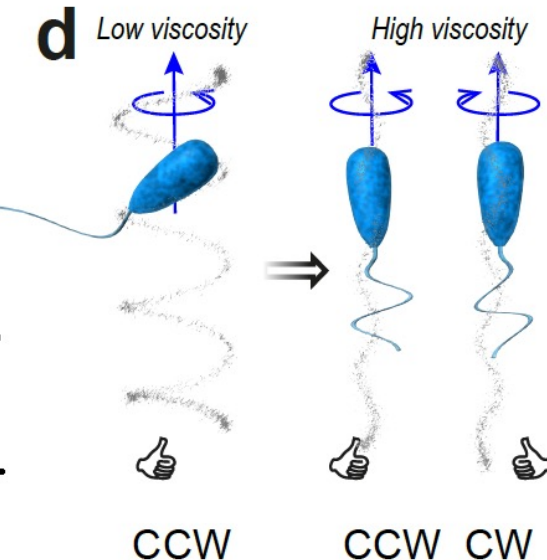
Elastohydrodynamic Coupling



Sperm Number

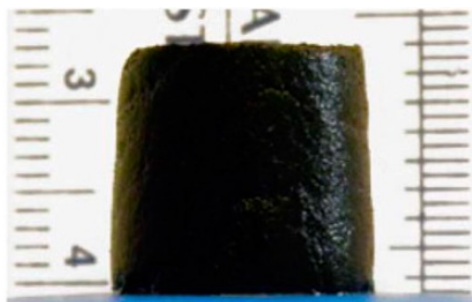
$$S_p = L / \left(\frac{\kappa}{\zeta_{\perp} \omega} \right)^{1/4}$$

Bending rigidity vs viscous drag



Ferrogels

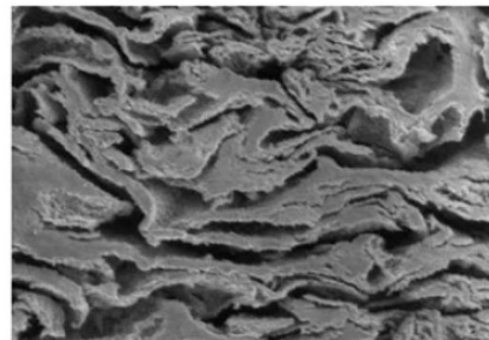
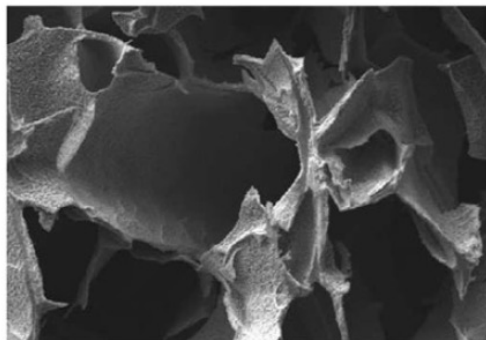
- Reduce elastic rigidity by creating macroscale pores inside the gel
- Reversible deformation with compressive strain over 80% before fracture
- Deformation under nonuniform magnetic fields
 - Body force proportional to the gradient of the applied field



C Field off

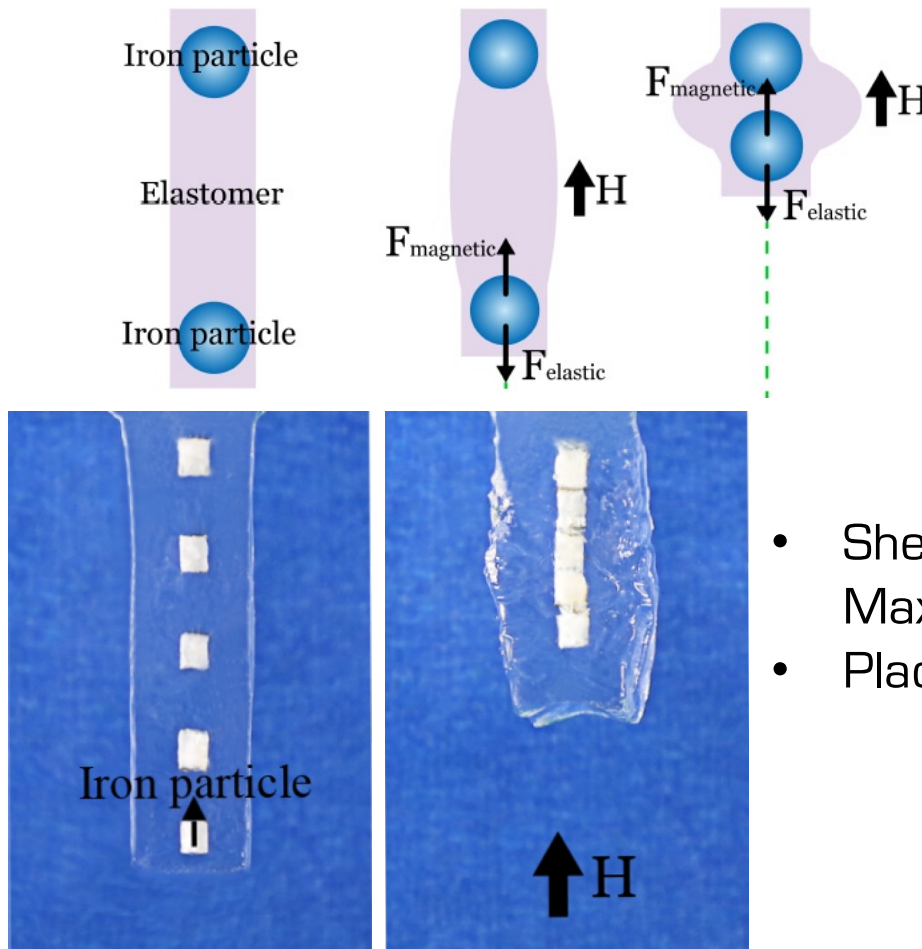


$$\mathbf{F} = \nu (\mathbf{M} \cdot \nabla) \mathbf{B}$$



Magnetoelastic Effect

- Magnetic pull-in instability



Magnetic Force

$$F_m \approx 3\mu_0 m^2 / (2\pi l^4)$$

$$m = V\chi_m H$$

Elastic Force (neo-Hookean)

$$F_e = A\gamma[l/l_0 - (l/l_0)^{-2}]$$

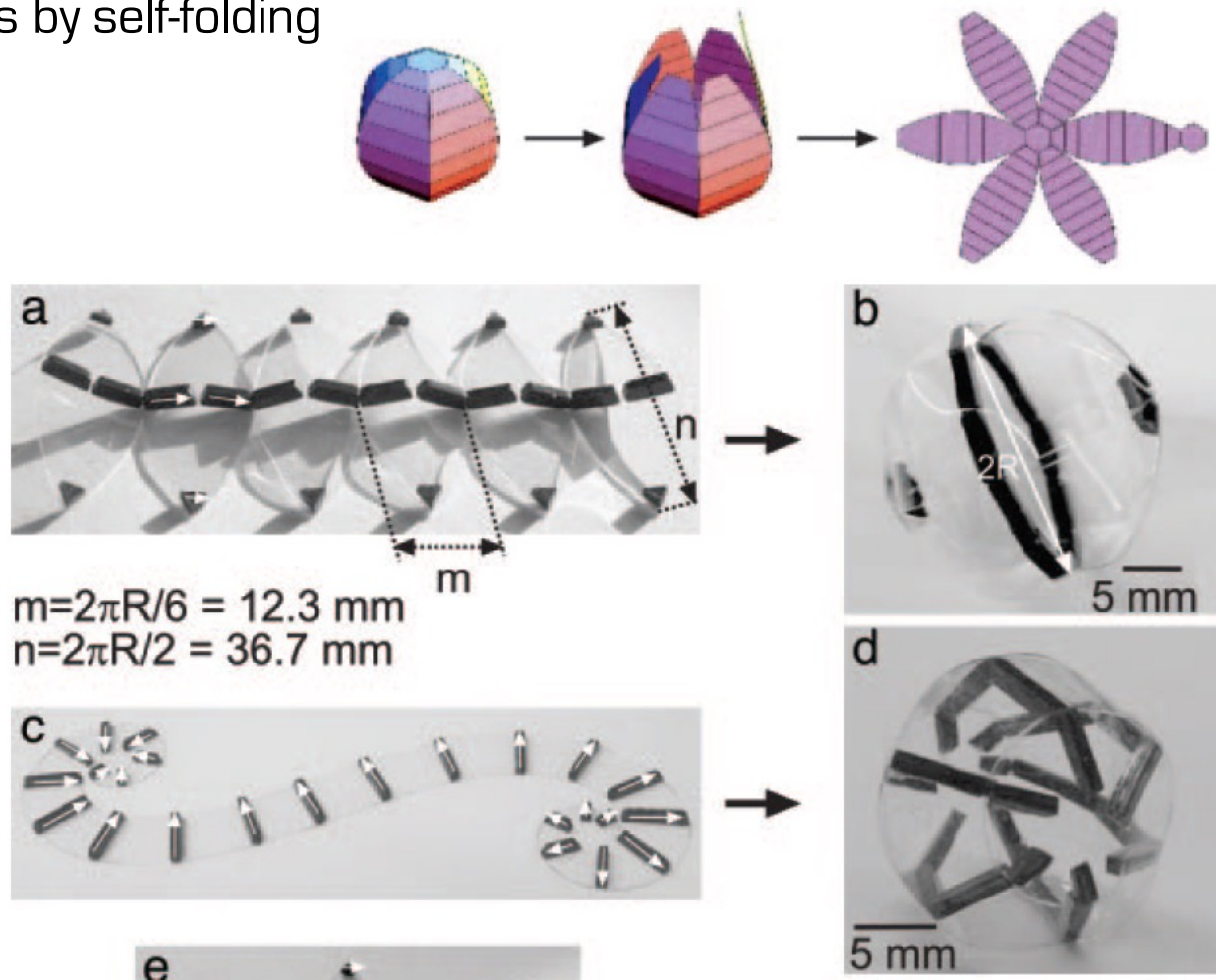
- Shear modulus of the matrix vs the magnetic Maxwell stress
- Placement of magnetic particles is the key

Hard Magnetic Composites

- Particles of high-coercivity ferromagnetic materials
 - Hard magnetic materials
 - such as NdFeB
- High remnant characteristics allow them to retain high residual magnetic flux density even in the absence of magnetic fields after saturation (high magnetization at low field)
- High coercivity helps them sustain high residual magnetic flux density over a wide range of applied magnetic fields below the coercive field strength (hard to demagnetize or re-magnetize)

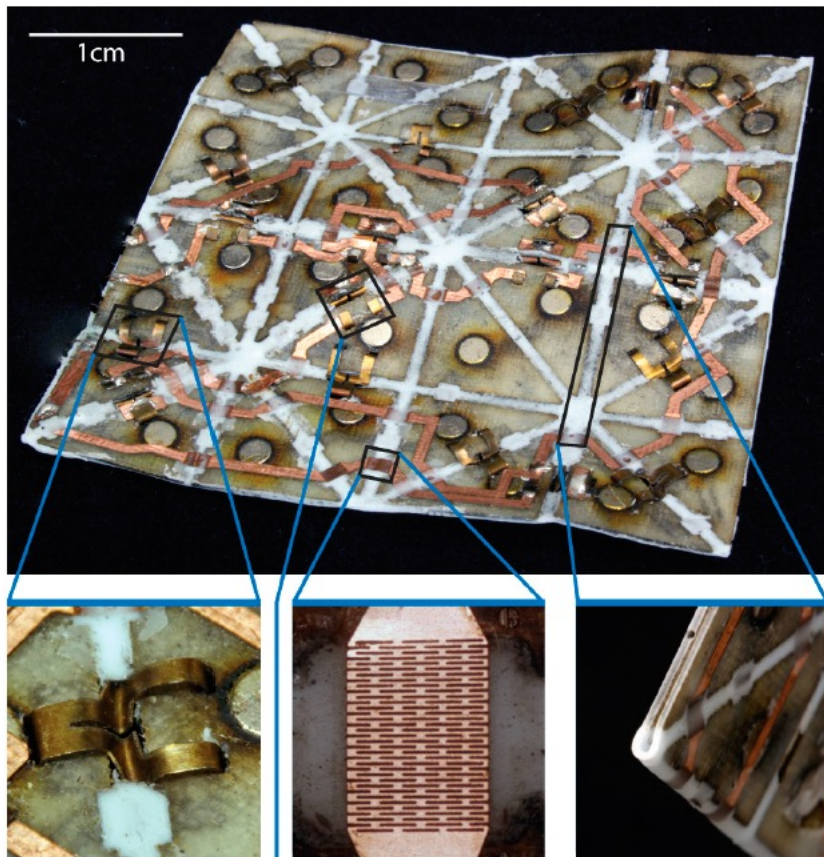
Magnetic self-assembly

- Converting elastomer sheets patterned with magnetic dipoles into 3D objects by self-folding



Programmable matter by folding

- Magnetic engagement for assembly



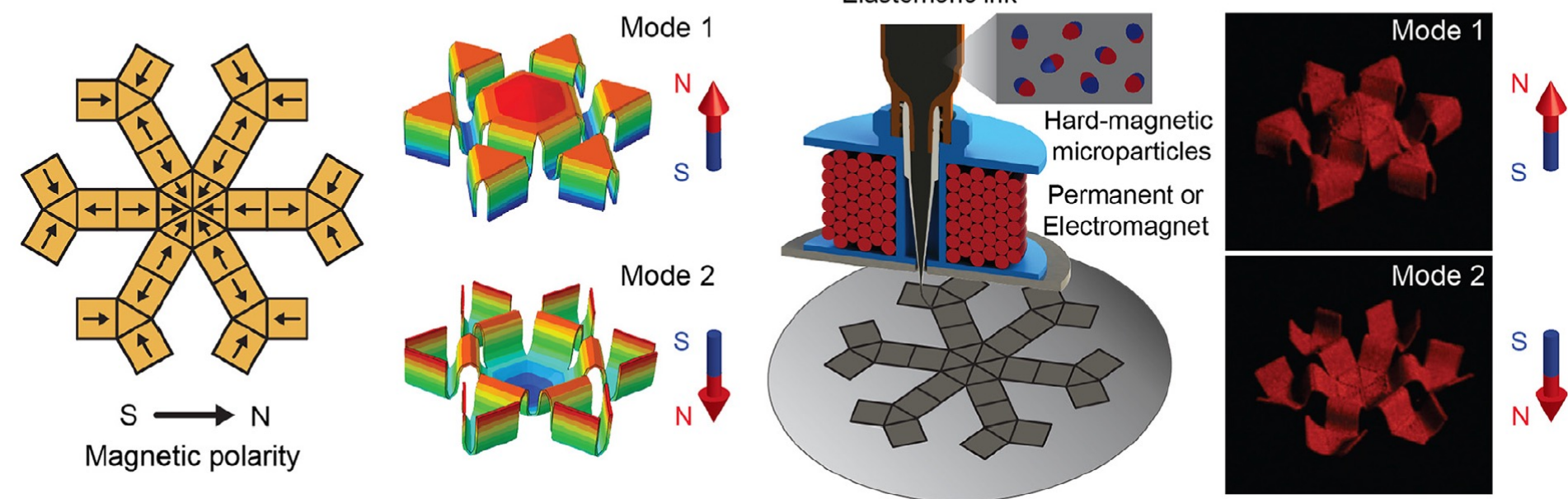
Programmable Matter by Folding

multiple shapes, compound folds

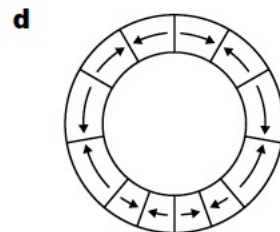
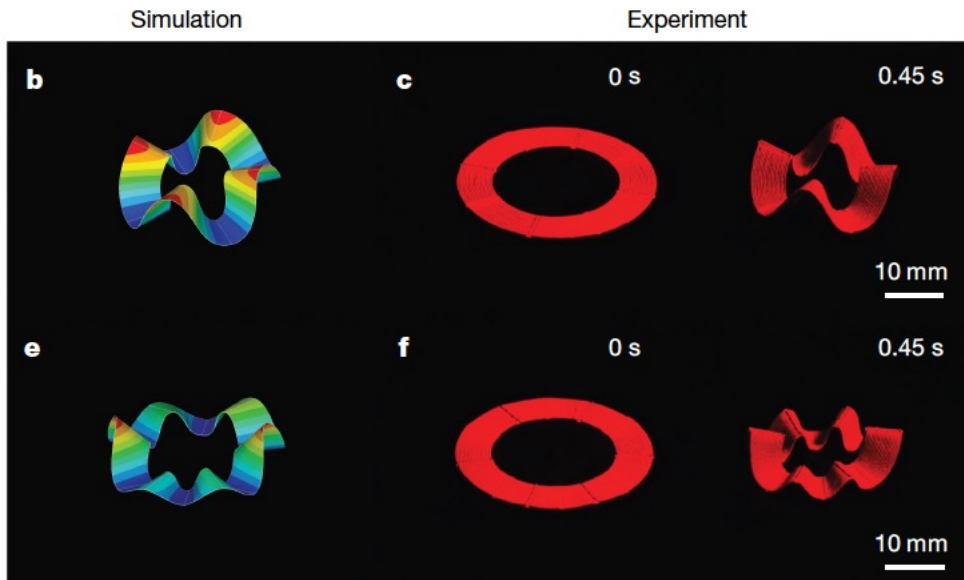
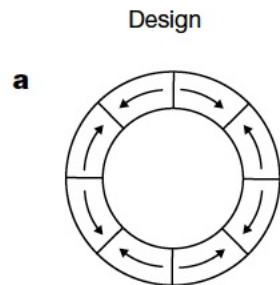
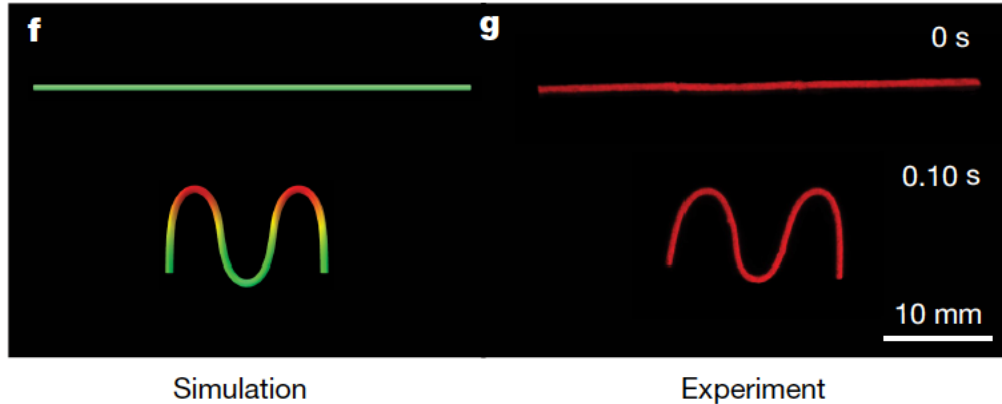
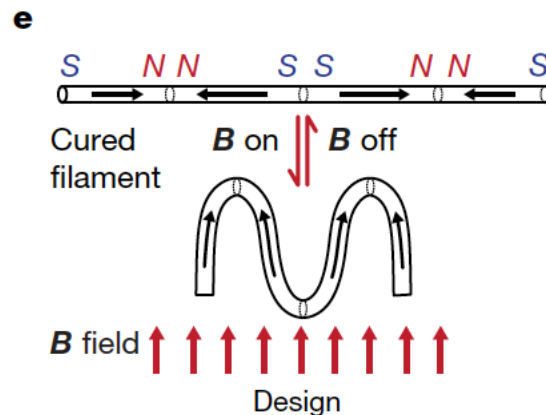
Hard Magnetic Composites

- Design of ferromagnetic domains in 3D printed soft materials

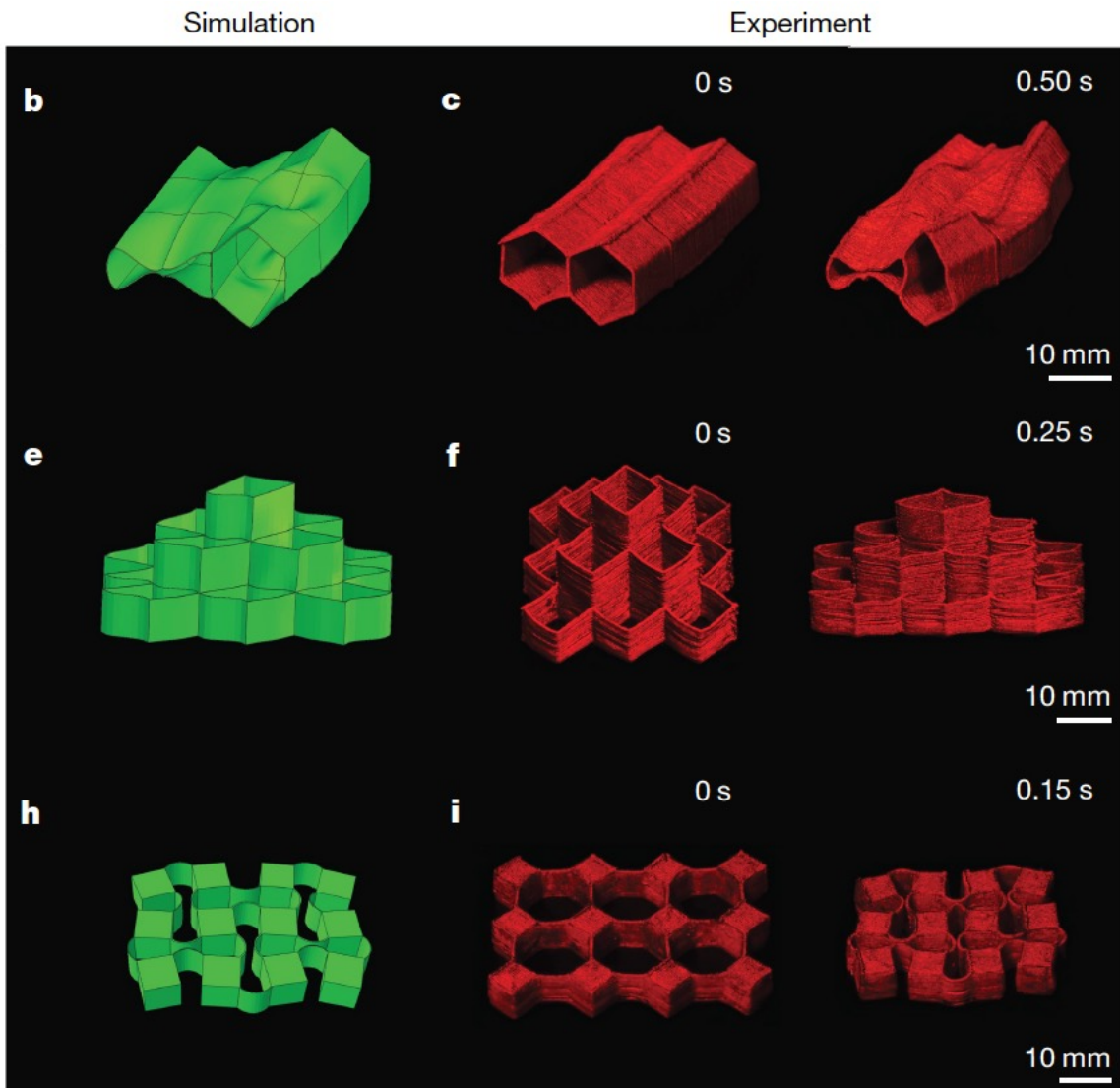
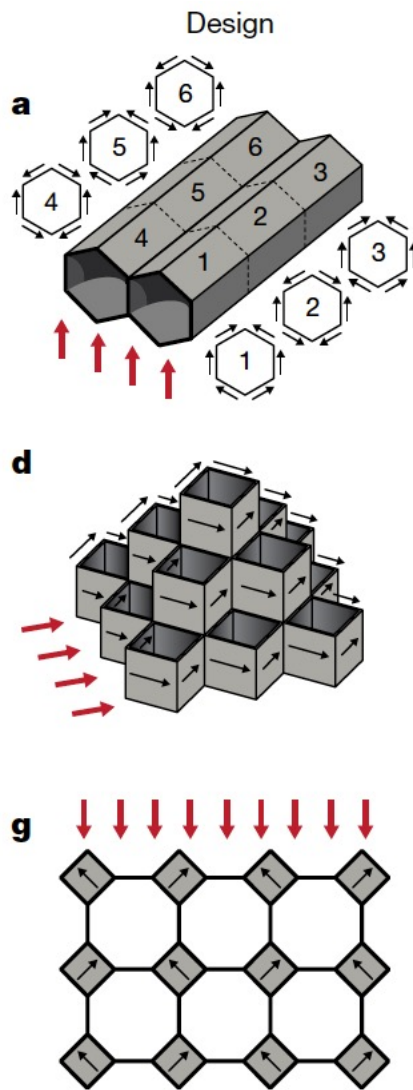
Design → Model-based Simulation → Fabrication (3D Printing) → Experiment



Hard Magnetic Composites



Hard Magnetic Composites



Hard Magnetic Composites

Printing ferromagnetic domains for untethered fast-transforming soft materials

Yoonho Kim^{1,2*}, Hyunwoo Yuk^{1*}, Ruike Zhao^{1*}, Shawn A. Chester³, Xuanhe Zhao^{1,4}

¹*Soft Active Materials Laboratory, Department of Mechanical Engineering, Massachusetts Institute of Technology*

²*Harvard-MIT Division of Health Sciences and Technology, Massachusetts Institute of Technology*

³*Department of Mechanical and Industrial Engineering, New Jersey Institute of Technology*

⁴*Department of Civil and Environmental Engineering, Massachusetts Institute of Technology*

*These authors contributed equally to the current work

Correspondence should be addressed to Xuanhe Zhao (zhaox@mit.edu)

Overall printing process and actuation of a shape-morphing structure with programmed ferromagnetic domains



Hard Magnetic Composites

Printing ferromagnetic domains for untethered fast-transforming soft materials

Yoonho Kim^{1,2*}, Hyunwoo Yuk^{1*}, Ruike Zhao^{1*}, Shawn A. Chester³, Xuanhe Zhao^{1,4}

¹*Soft Active Materials Laboratory, Department of Mechanical Engineering, Massachusetts Institute of Technology*

²*Harvard-MIT Division of Health Sciences and Technology, Massachusetts Institute of Technology*

³*Department of Mechanical and Industrial Engineering, New Jersey Institute of Technology*

⁴*Department of Civil and Environmental Engineering, Massachusetts Institute of Technology*

*These authors contributed equally to the current work

Correspondence should be addressed to Xuanhe Zhao (zhaox@mit.edu)

Fast transformation of a set of 2D structures into complex 3D shapes under applied magnetic fields



Hard Magnetic Composites

Printing ferromagnetic domains for untethered fast-transforming soft materials

Yoonho Kim^{1,2*}, Hyunwoo Yuk^{1*}, Ruike Zhao^{1*}, Shawn A. Chester³, Xuanhe Zhao^{1,4}

¹*Soft Active Materials Laboratory, Department of Mechanical Engineering, Massachusetts Institute of Technology*

²*Harvard-MIT Division of Health Sciences and Technology, Massachusetts Institute of Technology*

³*Department of Mechanical and Industrial Engineering, New Jersey Institute of Technology*

⁴*Department of Civil and Environmental Engineering, Massachusetts Institute of Technology*

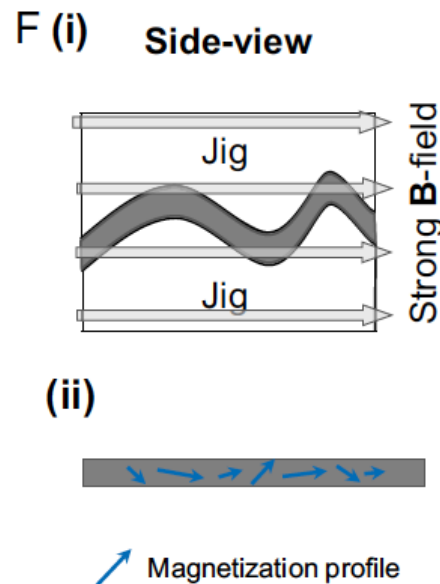
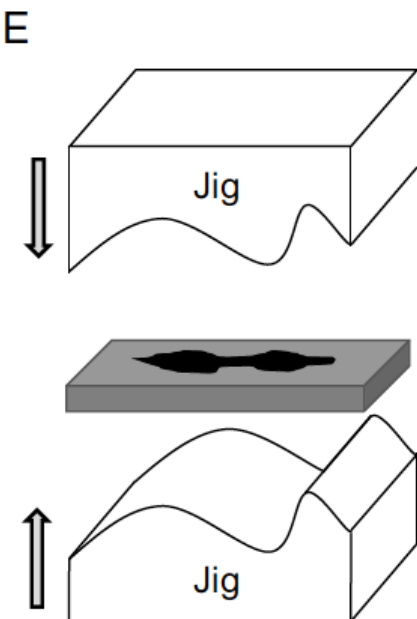
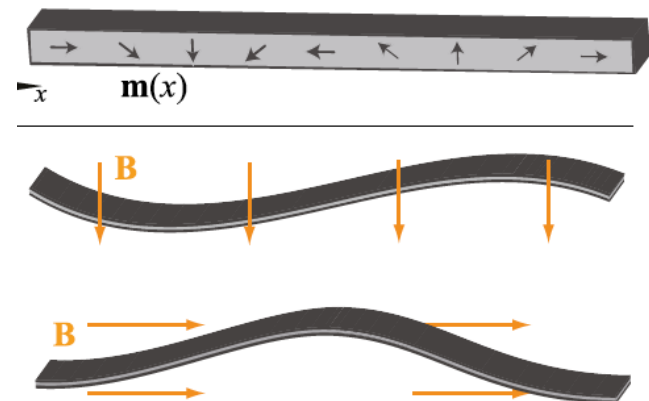
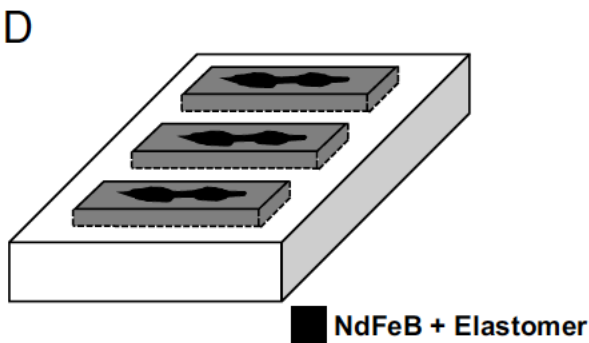
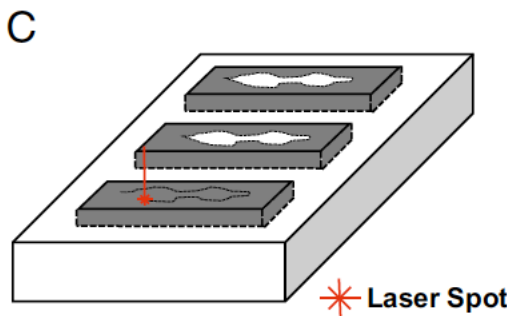
*These authors contributed equally to the current work

Correspondence should be addressed to Xuanhe Zhao (zhaox@mit.edu)

Rolling-based locomotion and delivery of a drug
pill of the hexapedal structure under a rotating
magnetic field



Shape-programmable magnetic soft matter

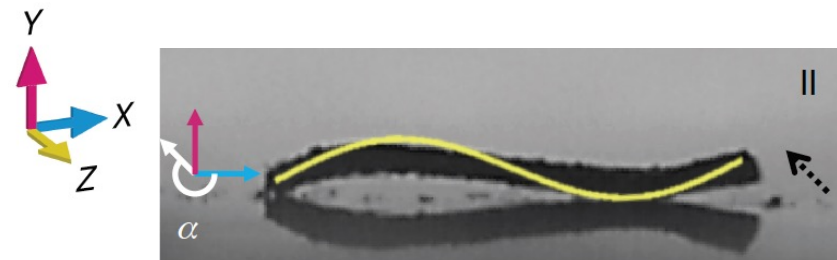
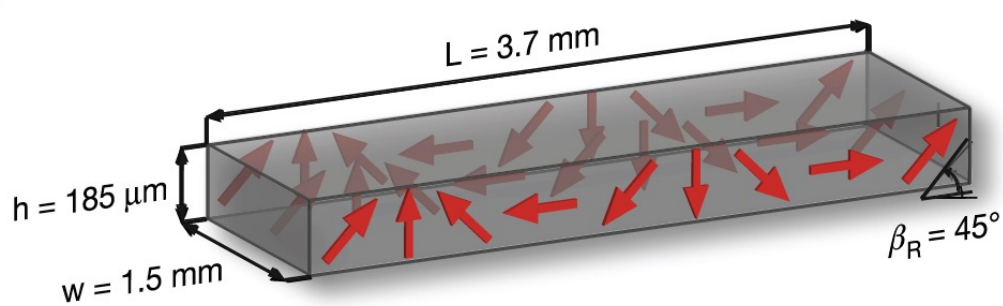


$$b = \frac{MA\lambda^3}{8\pi^3 EI} B$$

Shape-programmable magnetic soft matter

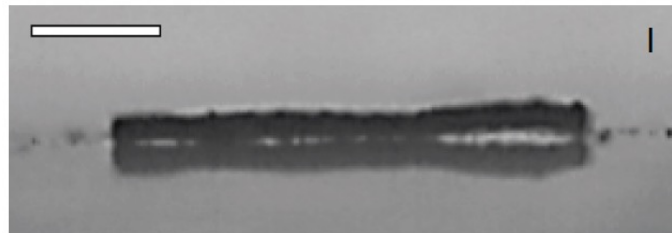
→ m → B → M_{net} — Model-predicted deflection

a

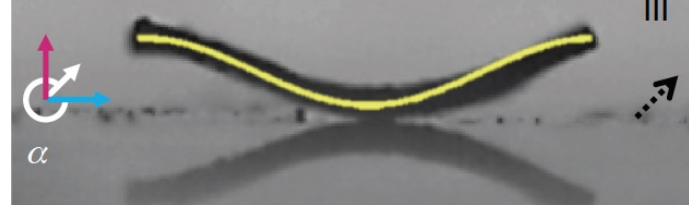


b

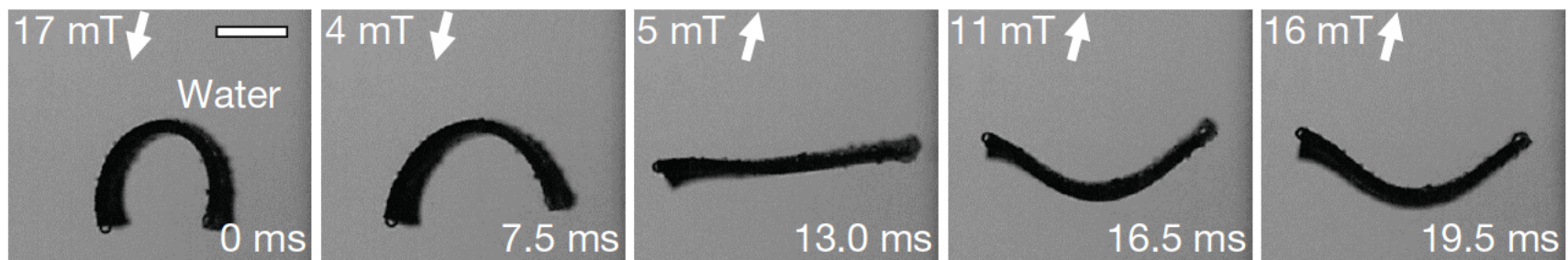
$$B_{xy} = 0$$



$$|M_{\text{net}}| = 0 \mu\text{A m}^2$$



Swimming



Small-scale soft-bodied robot with multimodal locomotion

Wenqi Hu, Guo Zhan Lum, Massimo Mastrangeli, Metin Sitti

Multimodal locomotion

(Play speed is indexed to real time)



Small-scale soft-bodied robot with multimodal locomotion

Wenqi Hu, Guo Zhan Lum, Massimo Mastrangeli, Metin Sitti

Cargo transport

(Play speed is indexed to real time)



Multi-functional soft-bodied jellyfish-like swimming

Ziyu Ren*, Wengi Hu*, Xiaoguang Dong, Metin Sitti**

-Biomimetic mode (Mode A)

(Play speed is indexed to real time)

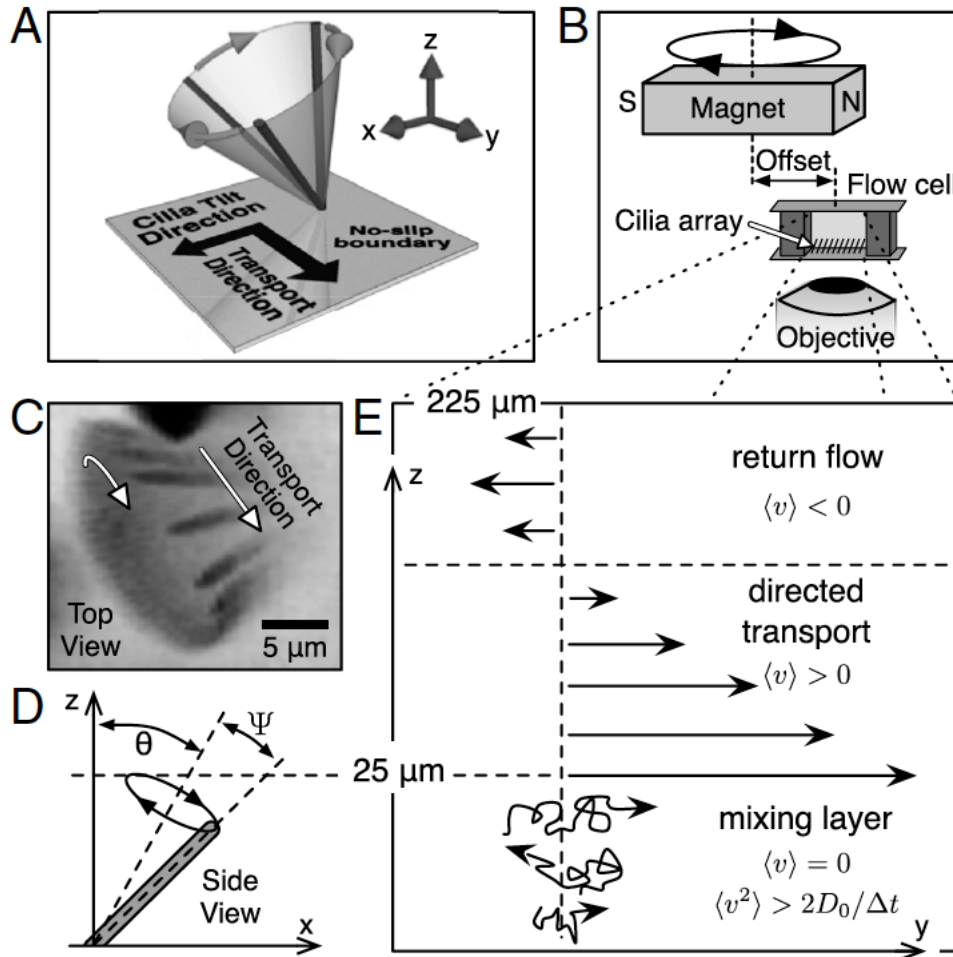
Magnetic Cilia Carpets with Programmable Metachronal Waves

**Supplementary video 1:
Metachronal waves with different wavelengths**

Hongri Gu, Quentin Boehler, Haoyang Cui, Eleonora Secchi, Giovanni Savorana, Carmela De Marco, Simone Gervasoni, Quentin Peyron, Salvador Pane, Tian-yun Huang, Ann Hirt, Daniel Ahmed, Bradley J. Nelson



Magnetically-actuated artificial cilia



Peclet Number

$$Pe = \frac{ul}{D_0}$$

u : characteristic velocity

l : characteristic length

D_0 : mass diffusivity

Stokes-Einstein

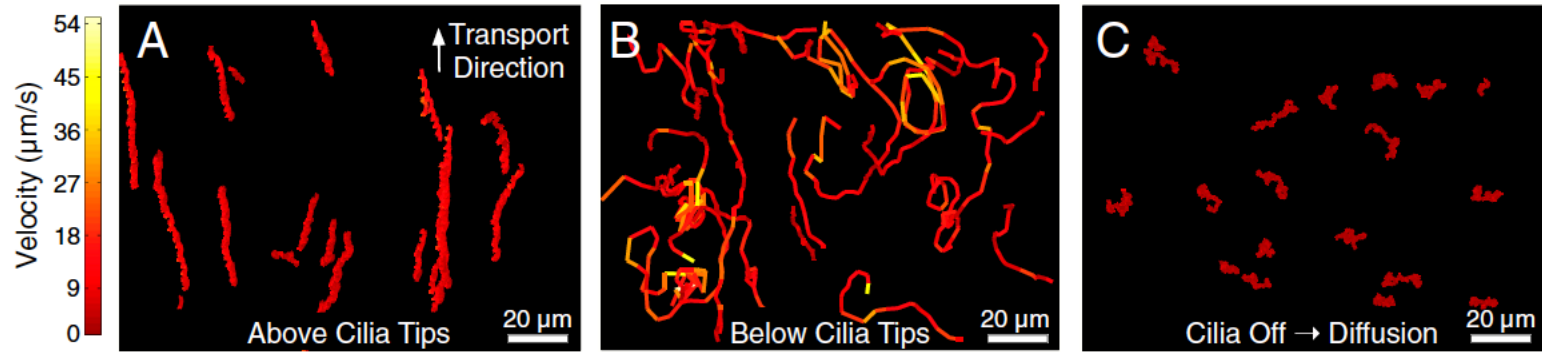
$$D_0 = \frac{kT}{3\pi\eta d} = 0.9 \text{ } \mu\text{m}^2/\text{s}$$

kT : thermal energy

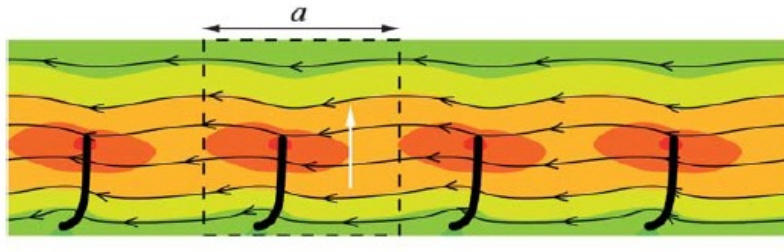
η : viscosity

d : diameter

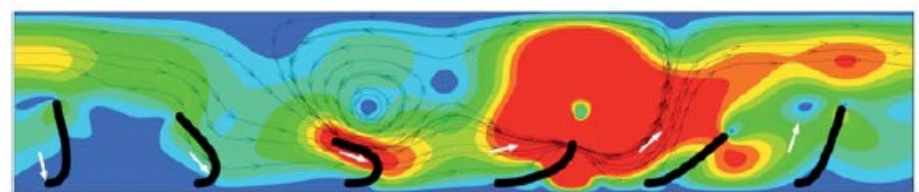
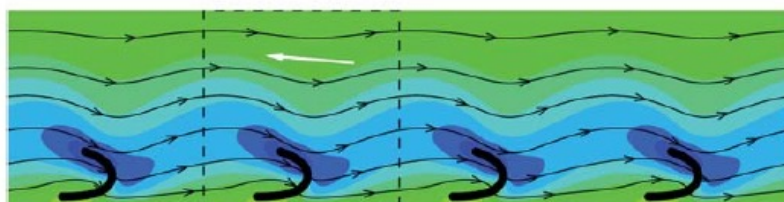
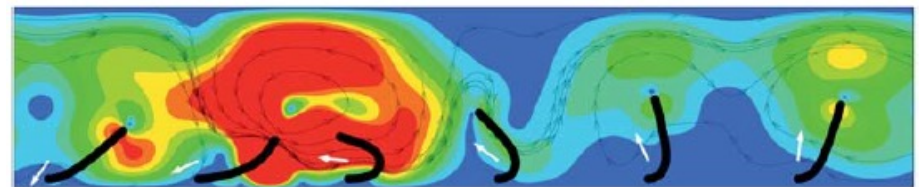
Magnetically-actuated artificial cilia



Synchronous beating



Out-of-phase movement



Magnetically-actuated artificial cilia

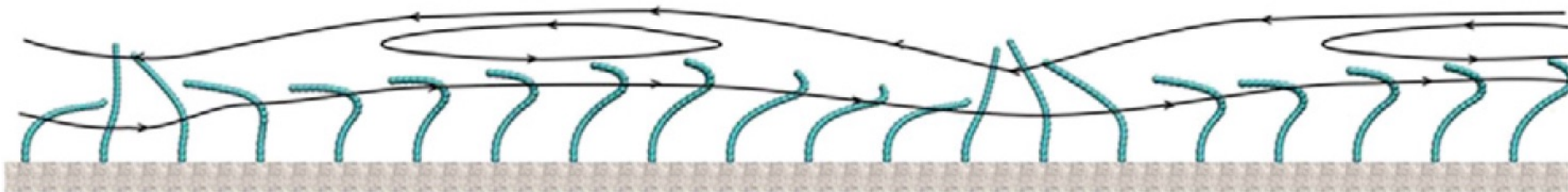
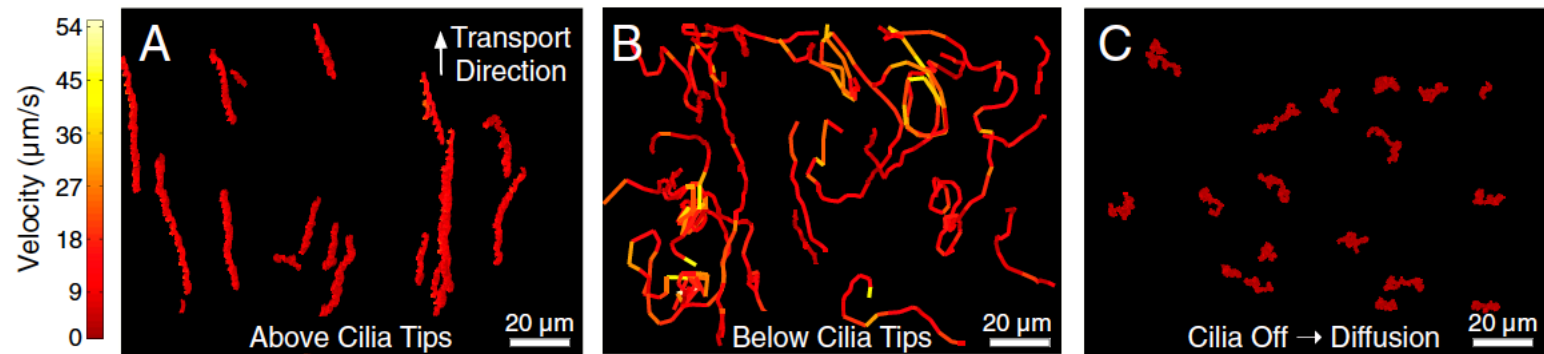
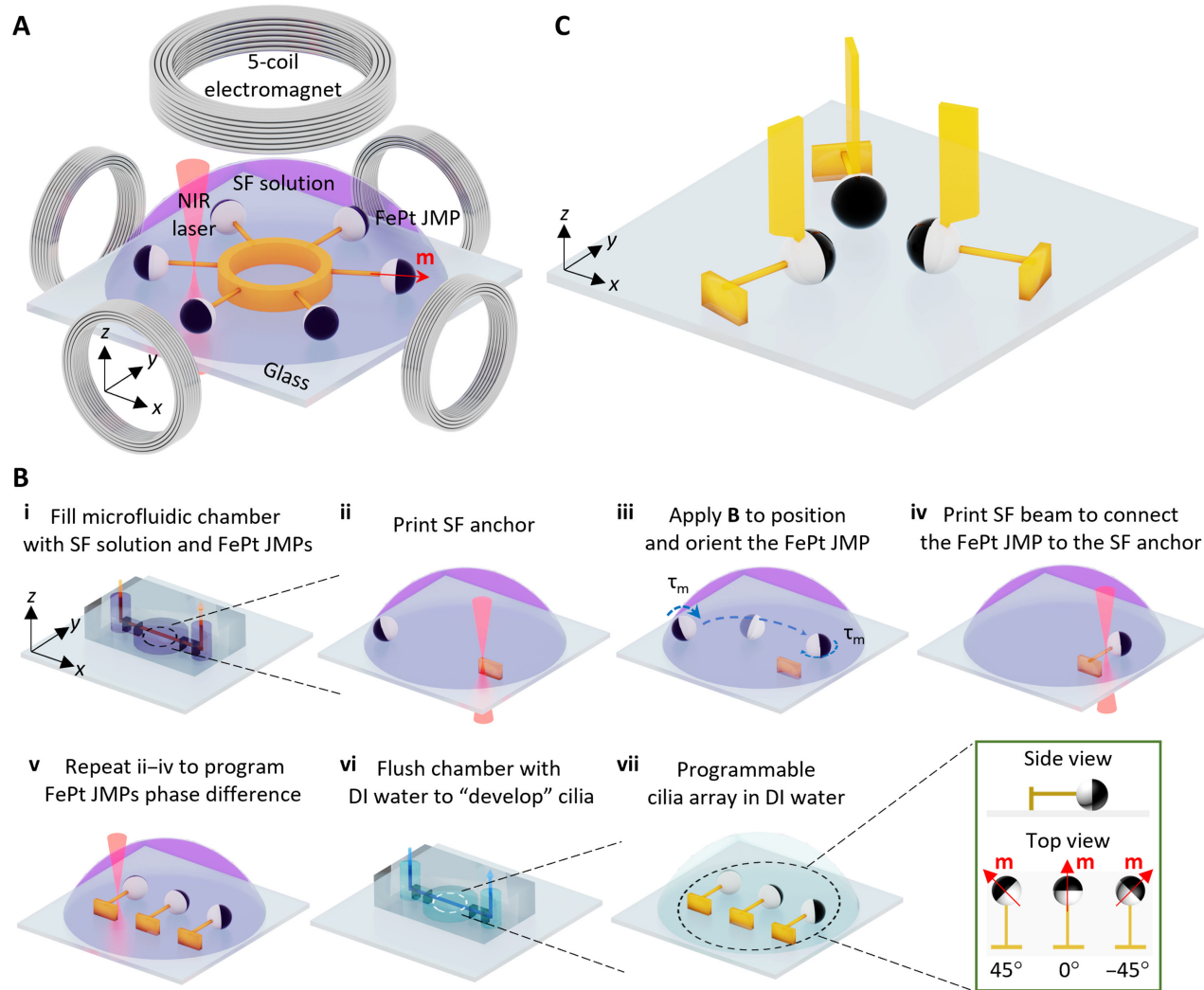


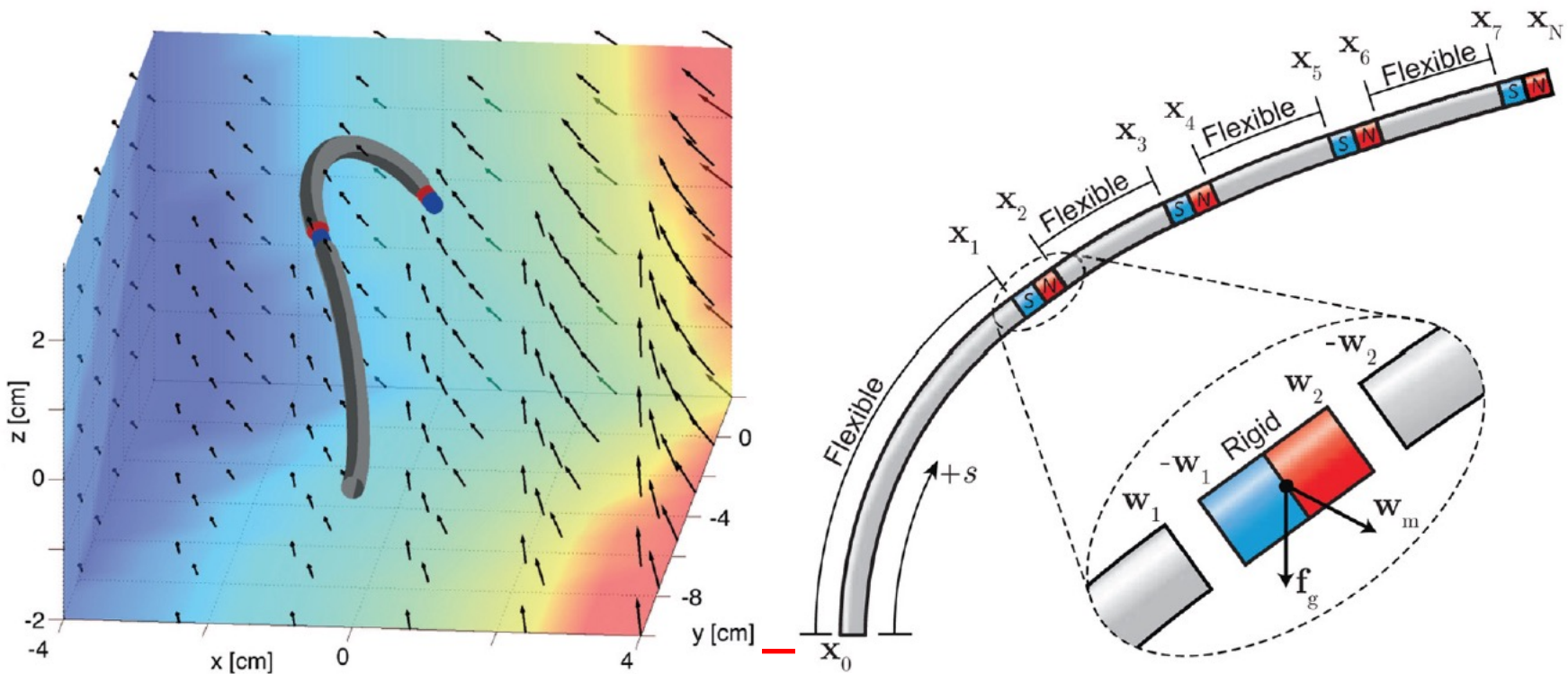
Fig. 5. Schematic view of metachronal beating to explain the origin of metachronal gain.

Magnetically-actuated artificial cilia



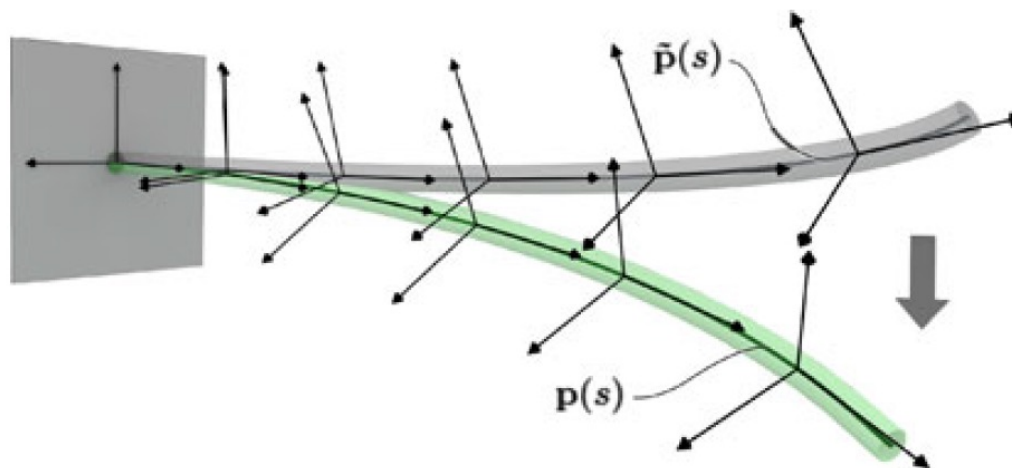
Magnetic control of continuum devices

- Guiding the translation and/or deformation of elastic rods
 - Surgical tasks with catheters
 - Do not require pull wires or other bulky mechanisms
 - Forces and torques generated by the interactions between embedded hard magnets and magnetic vector field



Magnetic control of continuum devices

- Rigid segments: standard rigid-body kinematics and force-torque equilibrium equations
- Flexible segments
 - Kirchhoff's theory: rod is not stretched, only bending strain
 - Cosserat-Timoshenko rod theory: with tensile and shear stiffness (flexibility of the rod in tension and shear)
 - Small strains and Hooke's law



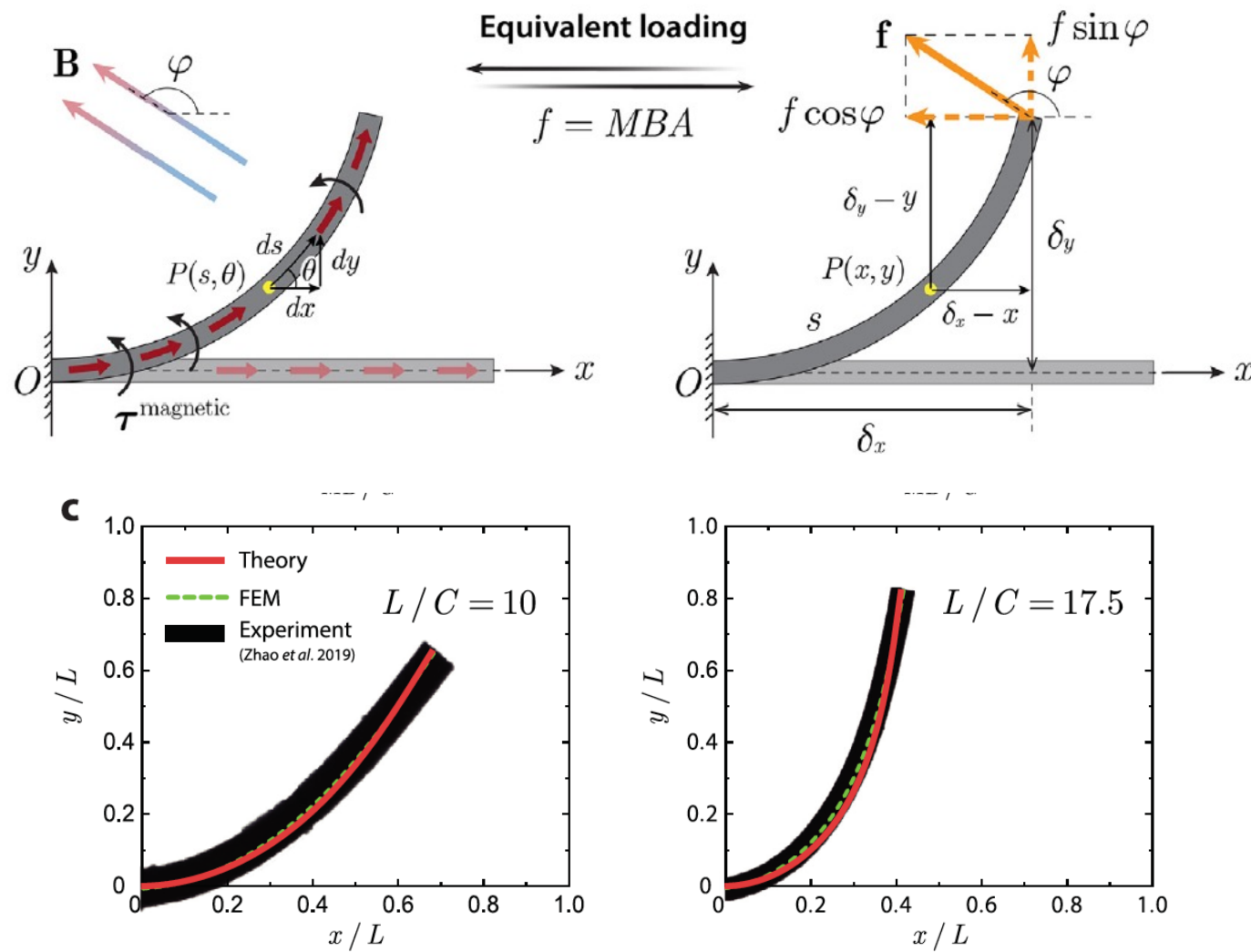
Hard-magnetic elastica

- Thin, elastic rod with hard magnetic properties
- Assumptions
 - cross-section remains perpendicular to the centerline of the body during deformation (i.e., no transverse shearing)
 - the centerline length of the elastica remains unchanged during deformation (i.e., centerline inextensibility along the length direction)
 - the incompressibility of constituent materials
 - the twisting motion has low practical implications for the interest in magnetically steerable soft continuum robots

$$\frac{EI}{A} \frac{d^2\theta}{ds^2} + MB \sin(\varphi - \theta) = 0$$

$$\frac{MBAL^2}{EI} = \frac{1}{2} \Phi^2(\varphi, \theta_L)$$

Hard-magnetic elastica



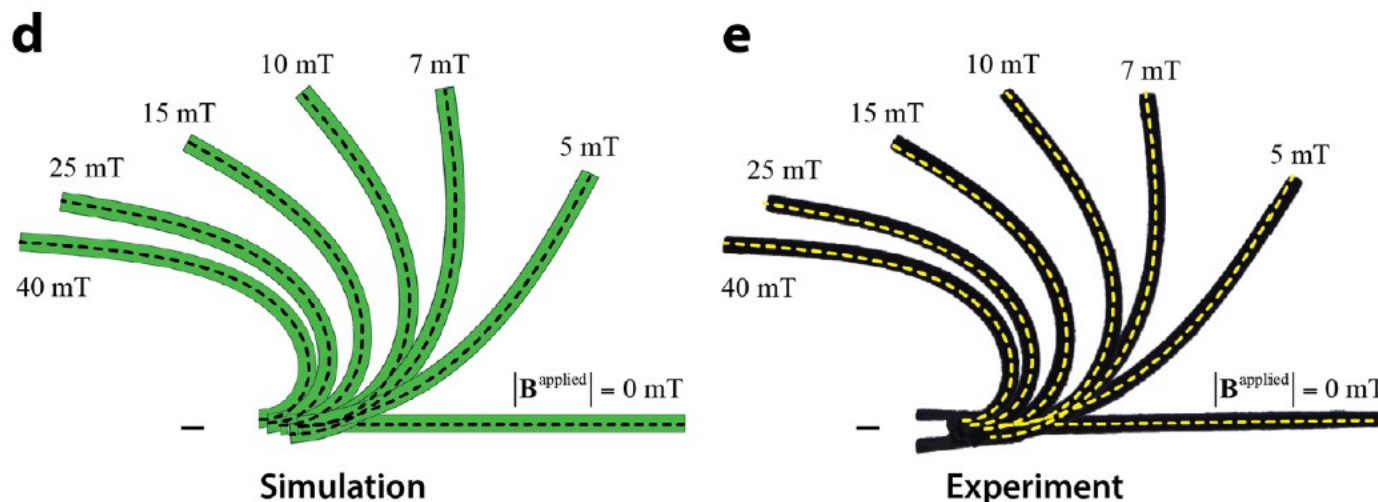
Finite element modeling

- Induced magnetic flux density exhibits a linear relation with applied magnetic field

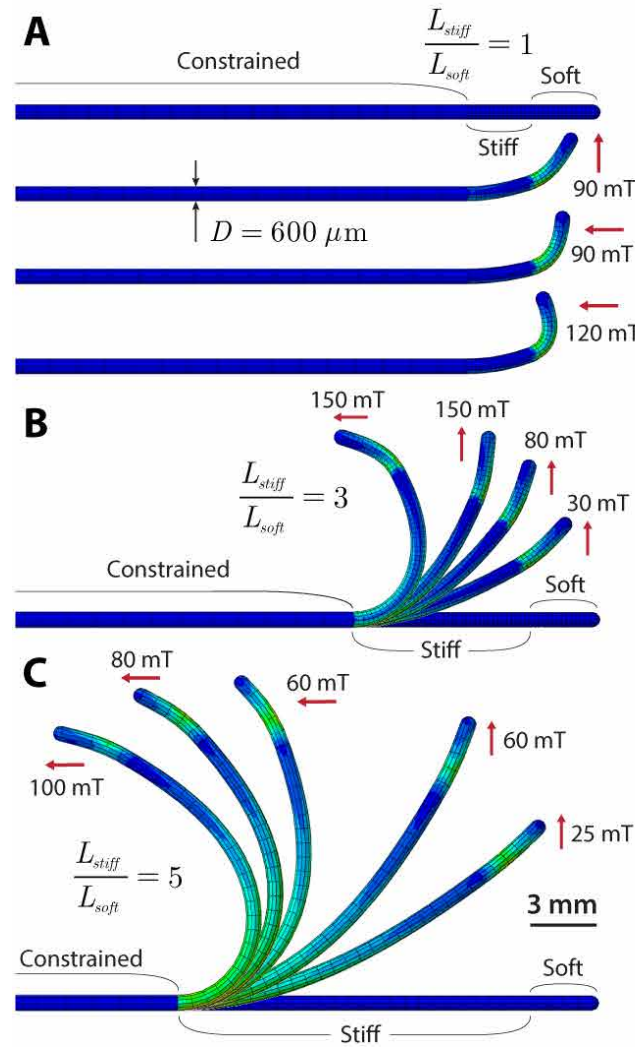
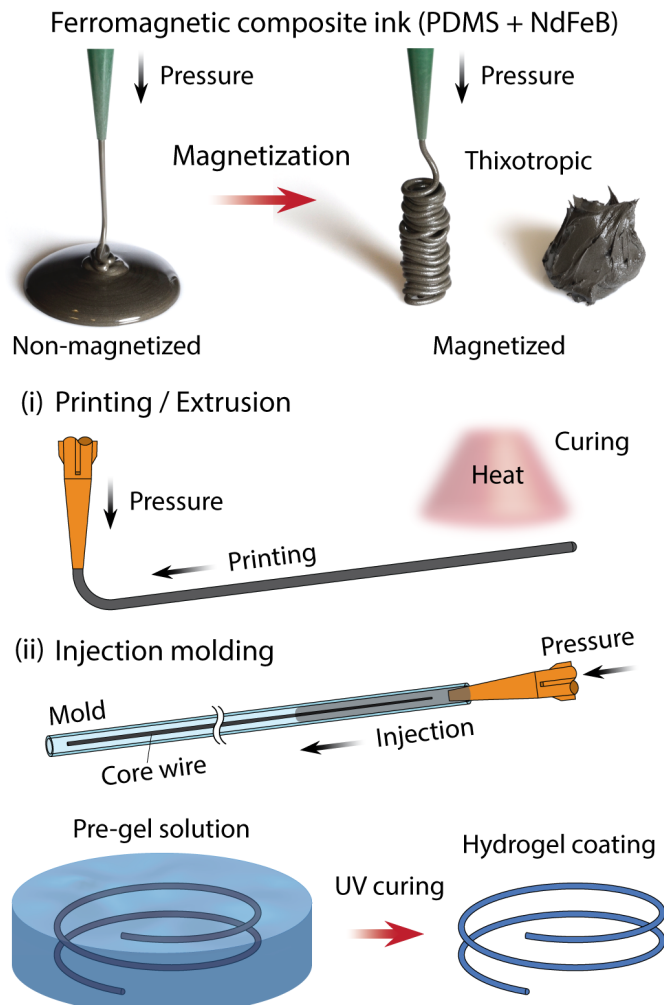
$$U = \underbrace{U_e(\mathbf{F})}_{\text{3D Elastic Energy}} + \underbrace{U_m(\mathbf{F}, \mathbf{B})}_{\text{Magnetic Potential}}$$

3D Elastic Energy Magnetic Potential

$$U_m = -\mathbf{F}\mathbf{M} \cdot \mathbf{B}$$



3D printed magnetic catheters



3D printed magnetic catheters

Ferromagnetic soft continuum robots

Yoonho Kim¹, German A. Parada^{1,2}, Shengduo Liu¹, Xuanhe Zhao^{1,3*}

¹*Department of Mechanical Engineering, Massachusetts Institute of Technology*

²*Department of Chemical Engineering, Massachusetts Institute of Technology*

³*Department of Civil and Environmental Engineering, Massachusetts Institute of Technology*

*Correspondence should be addressed to Xuanhe Zhao (zhaox@mit.edu).

Movie S3.

Ferromagnetic soft continuum robot navigating through a highly nonlinear path based on multiple modes and degrees of actuation.



Massachusetts
Institute of
Technology



Kim et al., *Sci. Robot.* **4**, eaax7329 (2019)

3D printed magnetic catheters

Ferromagnetic soft continuum robots

Yoonho Kim¹, German A. Parada^{1,2}, Shengduo Liu¹, Xuanhe Zhao^{1,3*}

¹*Department of Mechanical Engineering, Massachusetts Institute of Technology*

²*Department of Chemical Engineering, Massachusetts Institute of Technology*

³*Department of Civil and Environmental Engineering, Massachusetts Institute of Technology*

*Correspondence should be addressed to Xuanhe Zhao (zhaox@mit.edu).

Movie S6.

Comparison of the navigating performance: ferromagnetic soft continuum robots vs commercial guidewires with passive steering.



Kim et al., *Sci. Robot.* **4**, eaax7329 (2019)

Reprogramming magnetic properties

